Theory and Analysis of Quartz Crystal Resonators

A Tutorial at the 2010 IEEE International Frequency Control Symposium

by

Professor Yook-Kong Yong
Department of Civil & Environmental Engineering
Rutgers University
yong@rci.rutgers.edu
&
Professor Ji Wang
Piezoelectric Device Laboratory
School of Mechanical Engineering and Mechanics, Ningbo University
wangji@nbu.edu.cn

Outline

1. History and trends of quartz crystal resonators
2. Fundamentals of wave propagation
3. Quartz crystal material
4. Thickness vibrations of infinite plates
5. Mindlin plate equations
6. Complication factors
7. Analytical considerations
8. Finite element method

Part II

Part II

Yook-Kong Yong
Department of Civil & Environmental Engineering
Rutgers University
yong@rci.rutgers.edu

Analytical Considerations

1. 3-D piezoelectric equations for quartz with material dissipation
2. Butterworth Van Dyke resonator model of the quartz resonator: the equivalent electrical parameters
3. *Q* of a resonator
4. Eigenvalue analysis
5. Frequency response analysis

3-D piezoelectric equations for quartz *with* material dissipation

- Strain-displacement: $S_{ij} = \frac{1}{2}(U_{j,i} + U_{i,j})$
- Constitutive Equation: $T_{ij} = (C_{ijkl} + \boxed{j\omega\eta_{ijkl}})S_{kl} + e_{kij}\phi_{,k}$
- Electrostatic Constitutive Equation: $D_i = e_{ijk}S_{jk} - \varepsilon_{ik}\phi_{,k}$
- Stress equation of motion: $T_{ij,j} = -\omega^2 \rho U_i \text{ in } V$

  Specify $p_i = n_j T_{ij}$ or U_i in S
- Charge equation of motion: $D_{i,i} = 0 \text{ in } V$

  Specify $q = n_i D_i$ or ϕ in S

Butterworth Van Dyke resonator model of the quartz resonator

The resonator at rest is the shunt capacitor C_0

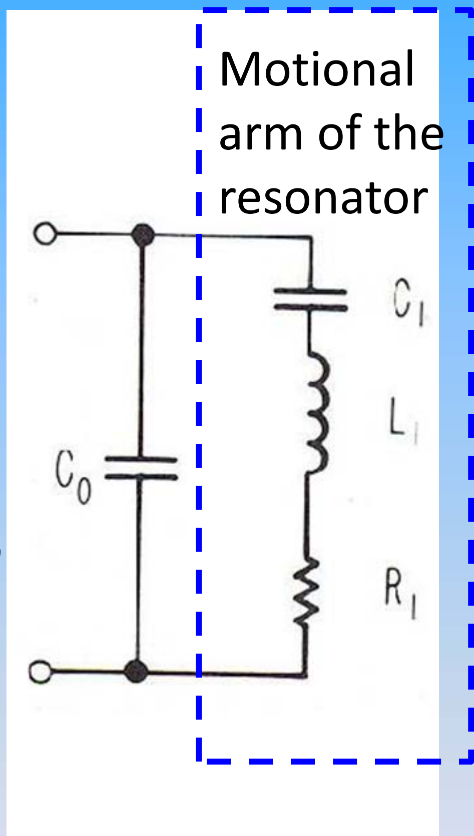

Harmonic excitation at frequency ω

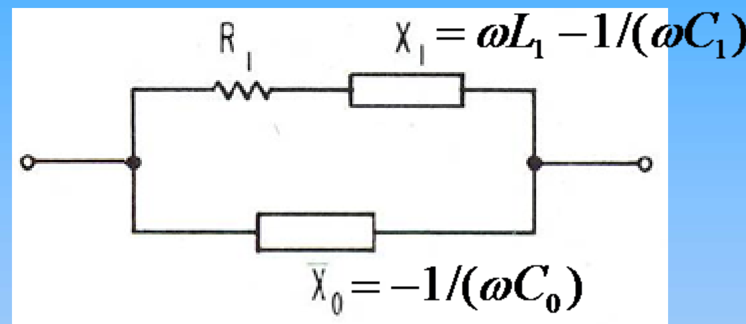

The inductance L_1 and reciprocal of motional capacitance $1/C_1$ represent respectively the effective mass and stiffness of the quartz resonator, while the resistance R_1 is the resonator damping

Ref: "Resonator and Device Measurements", E. Hafner, Precision Frequency Control Volume 2, Oscillators and Standards, Edited by E.A. Gerber and A. Ballato, Academic Press, Inc., 1985, Chapter 7, pp. 4-6.

Q of a resonator - 1

- There are demands for frequency devices with a low phase noise and high frequency stability based on a high *Q* factor. The devices are usually derived from the quartz crystal resonator.
- Rapid miniaturization of the quartz resonator causes a lowering of the *Q*.

Miniaturization trend of resonators

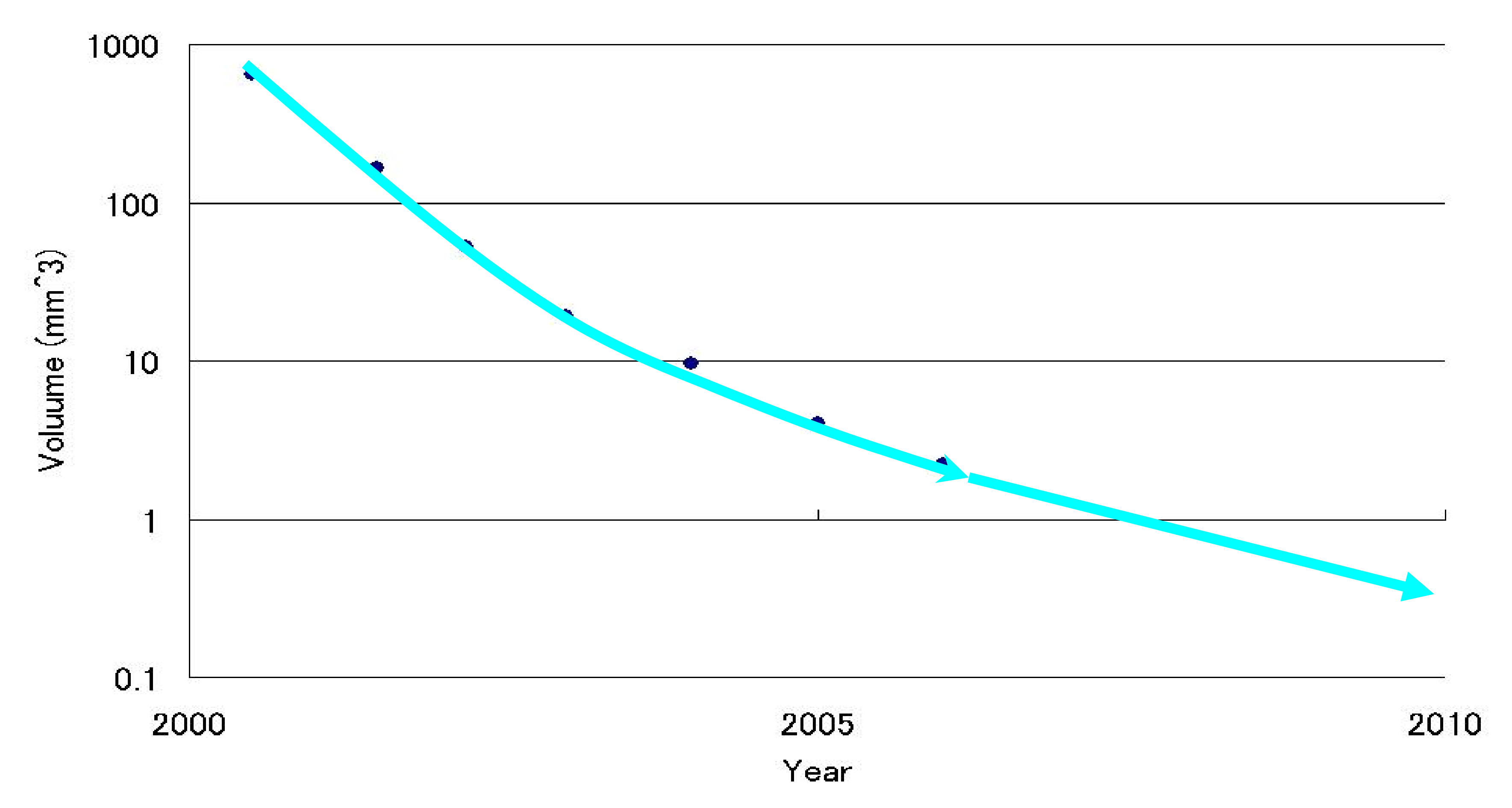

Q of a resonator - 2

- Good models are needed to reduce the cycle times for the design and prototyping of miniaturized resonators
- Accurate models for arriving at optimized designs of miniaturized quartz resonators along with an estimation of their *Q* and equivalent circuit parameters would be very useful.
- The miniaturized resonator is more sensitive to the effects of the packaging. Hence, 3-D models that include the effects of packaging are needed.

Possible factors that determine Q or R_1 of a resonator

1. Energy loss by mechanical viscosity
2. Friction loss at the interface between the electrode film and quartz plate
3. Electrical resistance along the lead pattern
4. Mechanical vibration loss through the supporting pads
5. Friction loss via the ambient gas
6. Coupling of the main mode with spurious modes

Eigenvalue analysis of quartz resonators with material dissipation and mounting substrate

Effects of an energy sink

2-D model of a high frequency mesa plate AT-cut quartz resonator mounted on a base

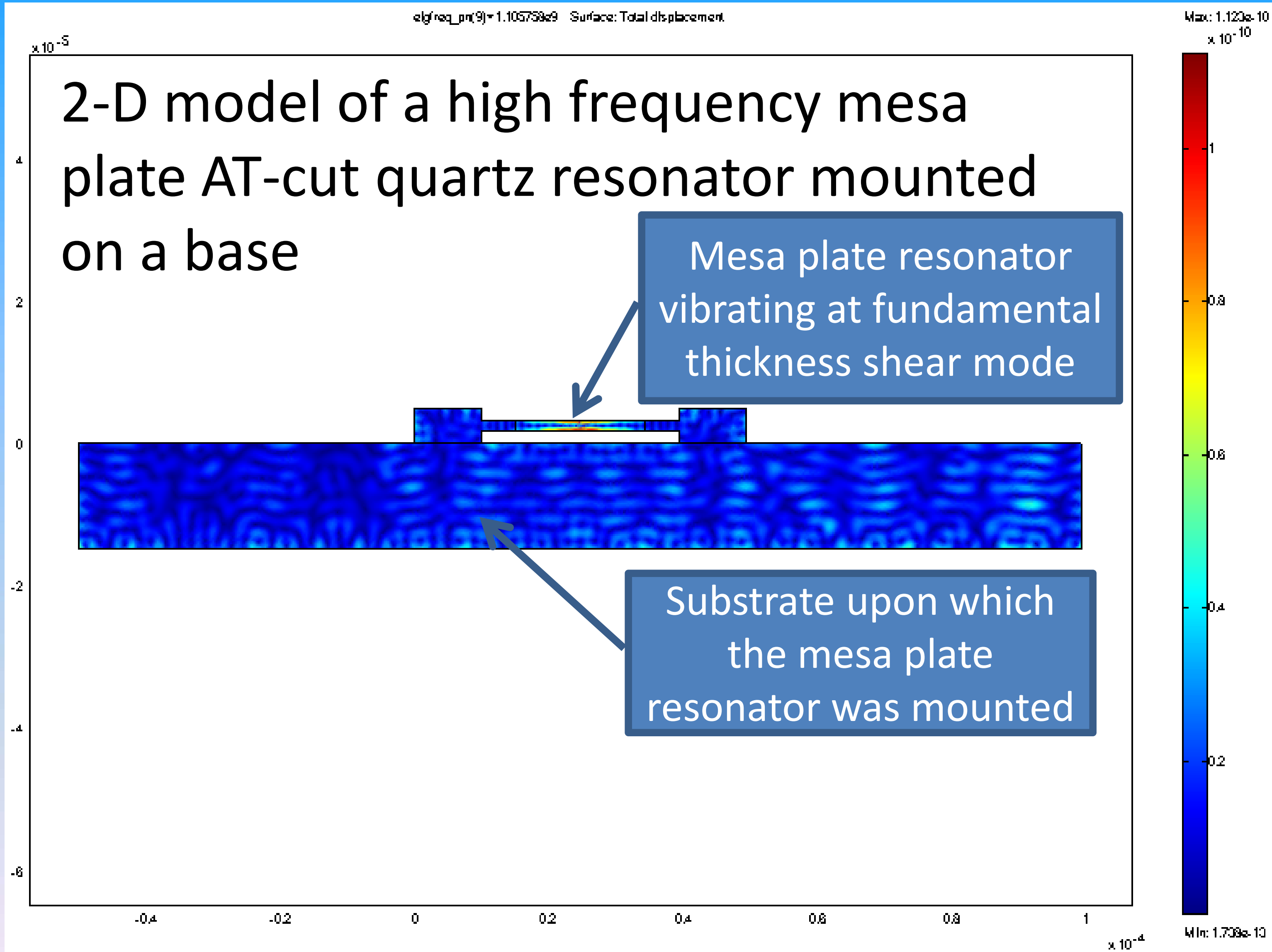

Comparison of frequency spectra using the 2-D model of the mesa plate AT-cut quartz resonator

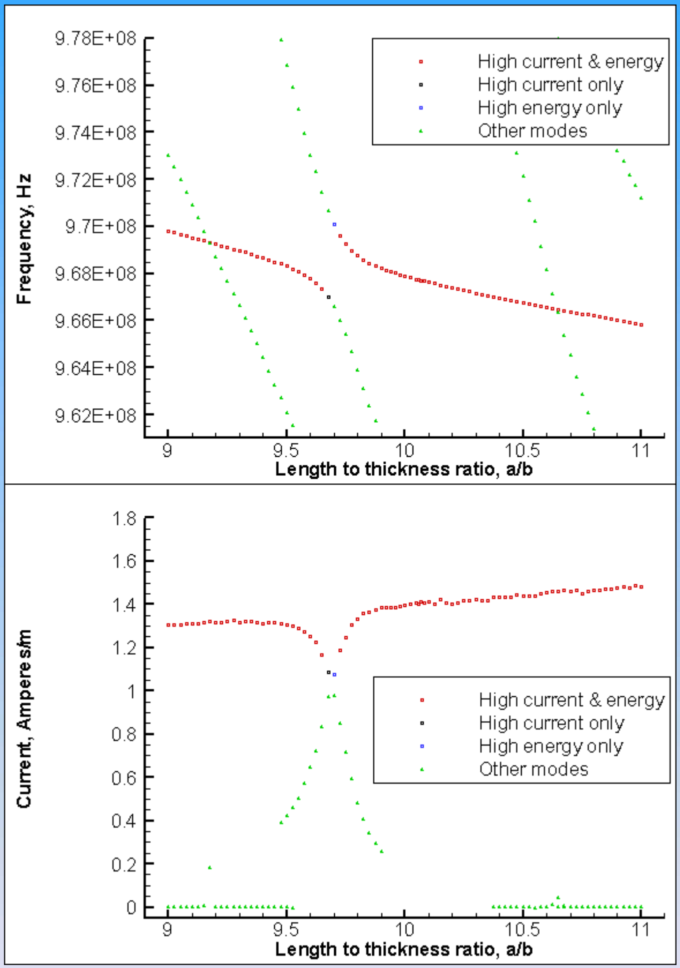

Mesa plate resonator itself

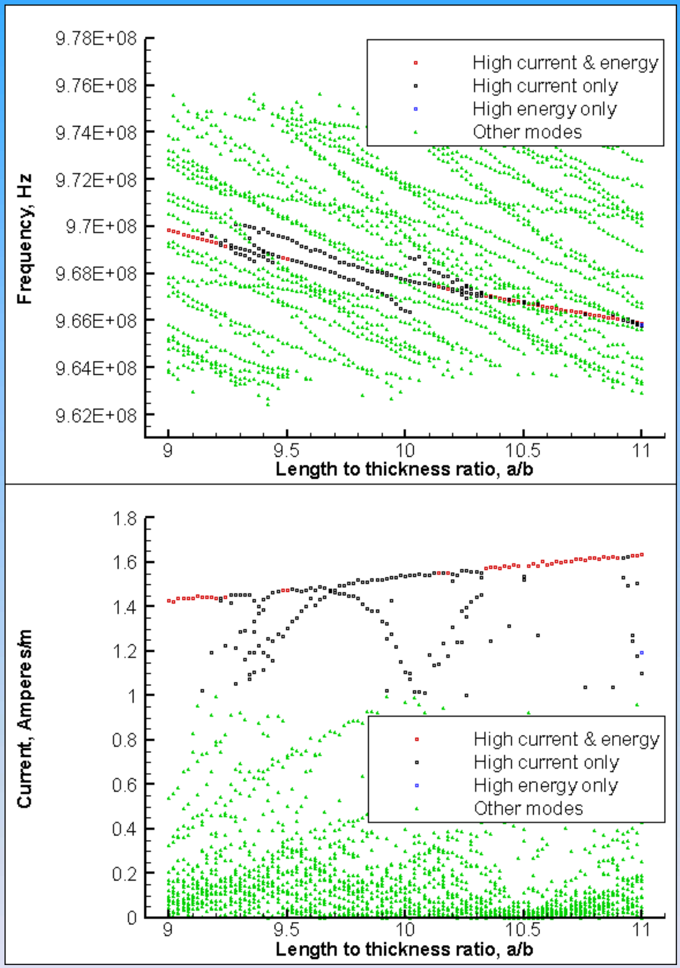

Mesa plate resonator mounted on the base

The frequency spectrum of the mesa plate resonator mounted on a base substrate is much richer, hence there will be more interactions with spurious modes that lead to lower *Q* factors

Dimensions of the AT-cut quartz resonator

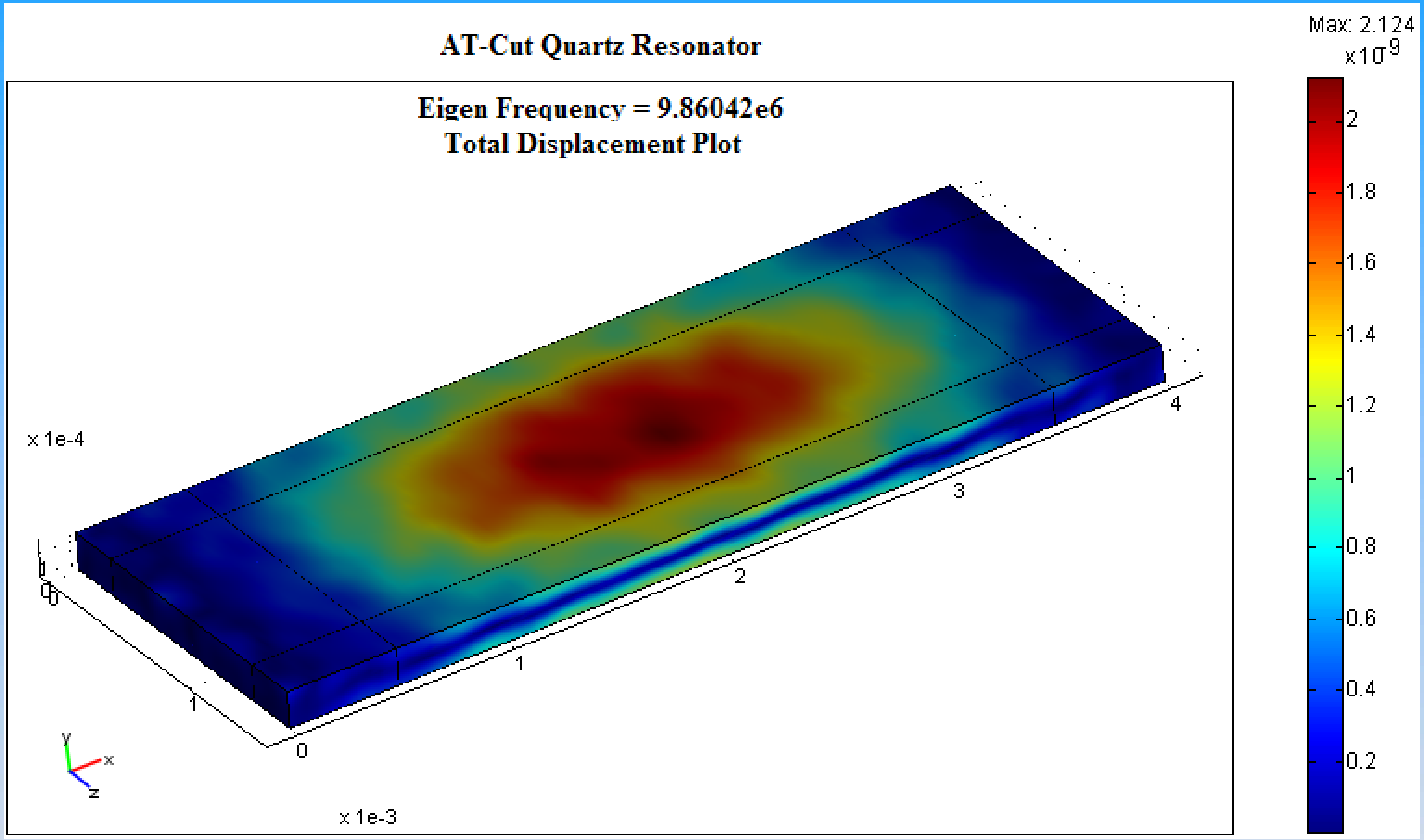

Blank: 4000 microns (X1) x 1500 microns (X3) x 165.47 microns (X2)

Gold Electrodes: 3000 microns (X1) x 1000 microns (X3) x 0.3 microns (X2)

10 MHz AT-cut quartz resonator with dissipation for a/b = 24-25

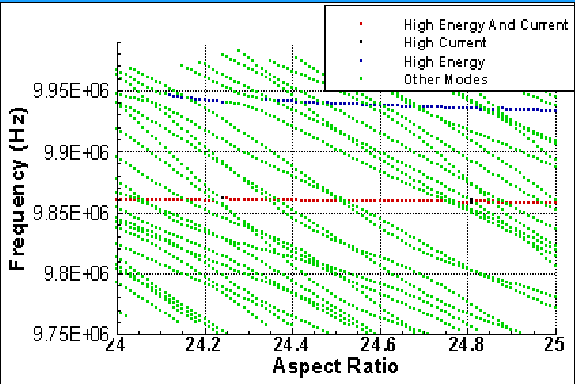

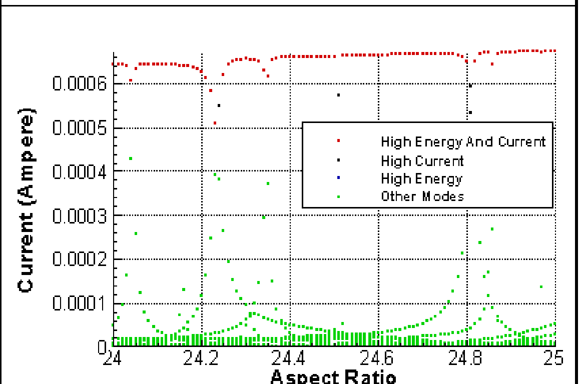

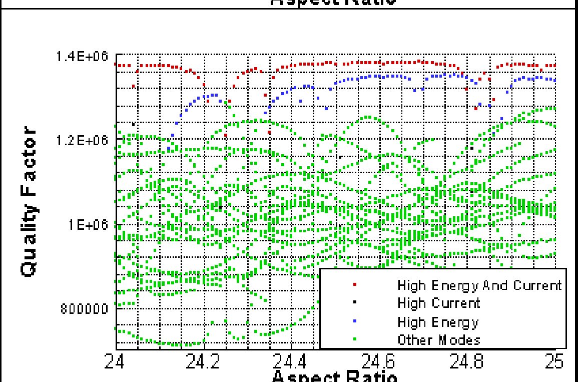

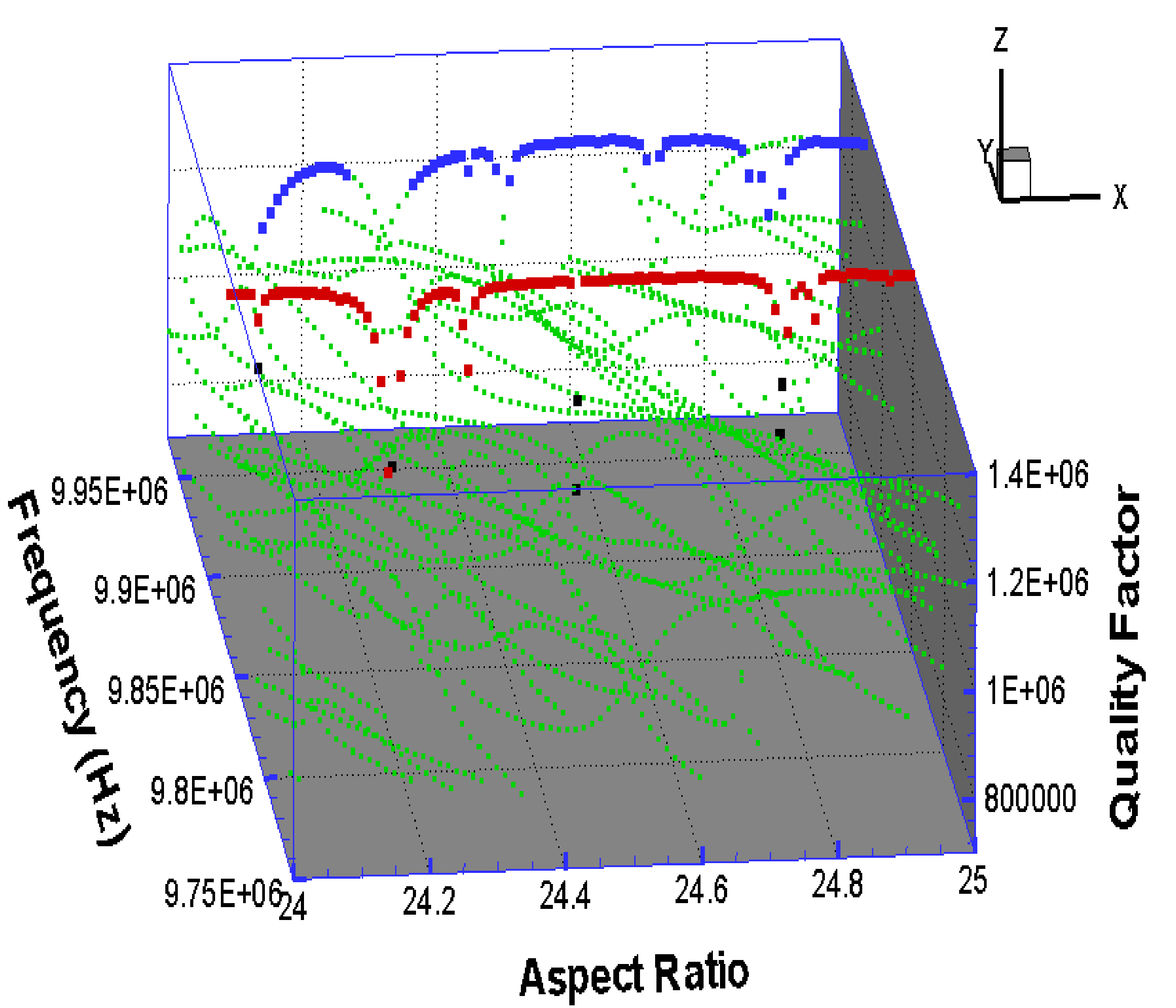

Eigenvalue analysis of two 12 MHz AT-cut resonators

A model of a 12 MHz AT-cut Quartz Resonator

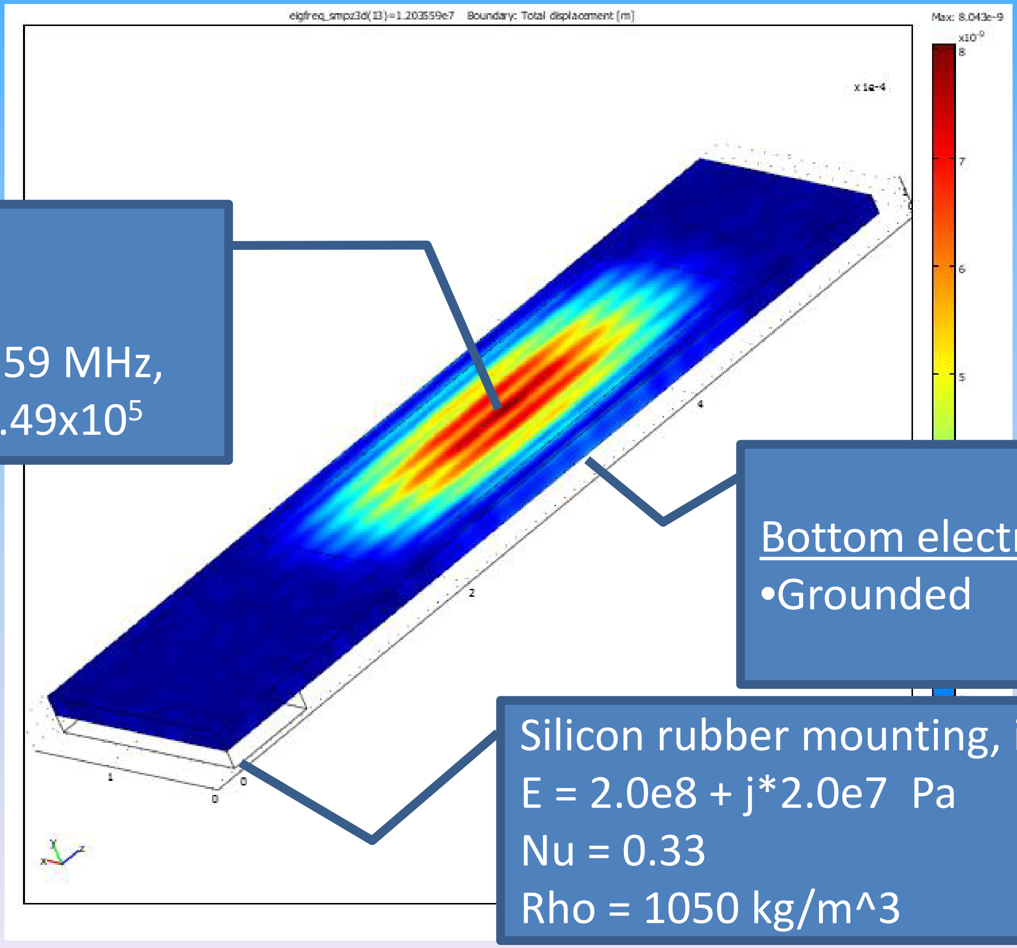

Top electrode

Grounded

f_R = 12.03559 MHz,

Qfactor = 1.49×10^5

Bottom electrode

•Grounded

Silicon rubber mounting, isotropic material:

E = 2.0e8 + j*2.0e7 Pa

Nu = 0.33

Rho = 1050 kg/m^3

Resonators A, and B
12 MHz AT-cut Quartz Resonators

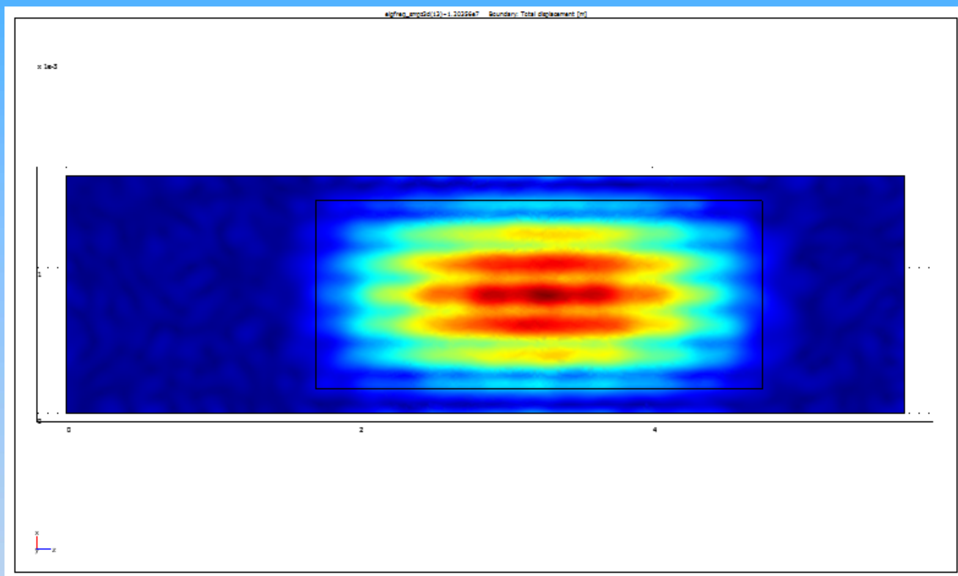

A: Blank: X=1627 um, Z=5715 um, Y=132.8 um
Electrode: X=1288 um, Z=3048 um, 0.5 um gold

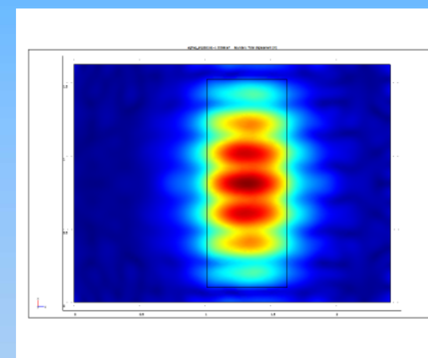

B: Blank: X=1627 um, Z=2413 um, Y=132.3 um
Electrode: X=1422 um, Z=635 um, 0.5 um gold

BVD electrical parameters by eigenvalue analysis

1) Obtain from eigenvalue analysis
   a) ω_R , real, short circuit resonance frequency, rad/s
   b) ω_I, imaginary, short circuit resonance frequency, rad/s

2) $Q = \omega_R /(2\, \omega_I)$

3) $$C_1 = \frac{I_m^2}{2\omega_R^2 E_{kin}} \quad \text{where} \quad E_{kin} = \frac{\omega_R^2}{2}\int_V \rho\,|u|^2\,dV\,,$$

   and I_m is the current over the top electrode

4) $R_1 = 1/[\omega_R\, QC_1]$ motional resistance

5) $L_1 = 1/[C_1\, \omega_R^2]$ motional inductance

6) C_0 = the total charge over the 1V top electrode in an electrostatic problem, bottom electrode grounded

12 MHz AT-Cut Thickness Shear Resonator

	Resonator A		Resonator B	
BVD parameters	Eigenvalue analysis	[1]Measured values	Eigenvalue analysis	[1]Measured values
f_r , MHz	12.03559	12.0	12.25664	12.0
[2]C_0 , pF	1.22	1.23	0.31	0.35
C_1 , fF	5.41	5.7	1.38	1.8
L_1 , mH	32.8	Not available	128.3	Not available
R_1 , ohm	16.6	15	130	< 1000

[1]Measured values provided by Statek, Inc.
[2]From piezo-electrostatic calculation

Frequency response analysis of quartz resonators with material dissipation and mounting substrate

Frequency response analysis for AT-Cut quartz with and without dissipation

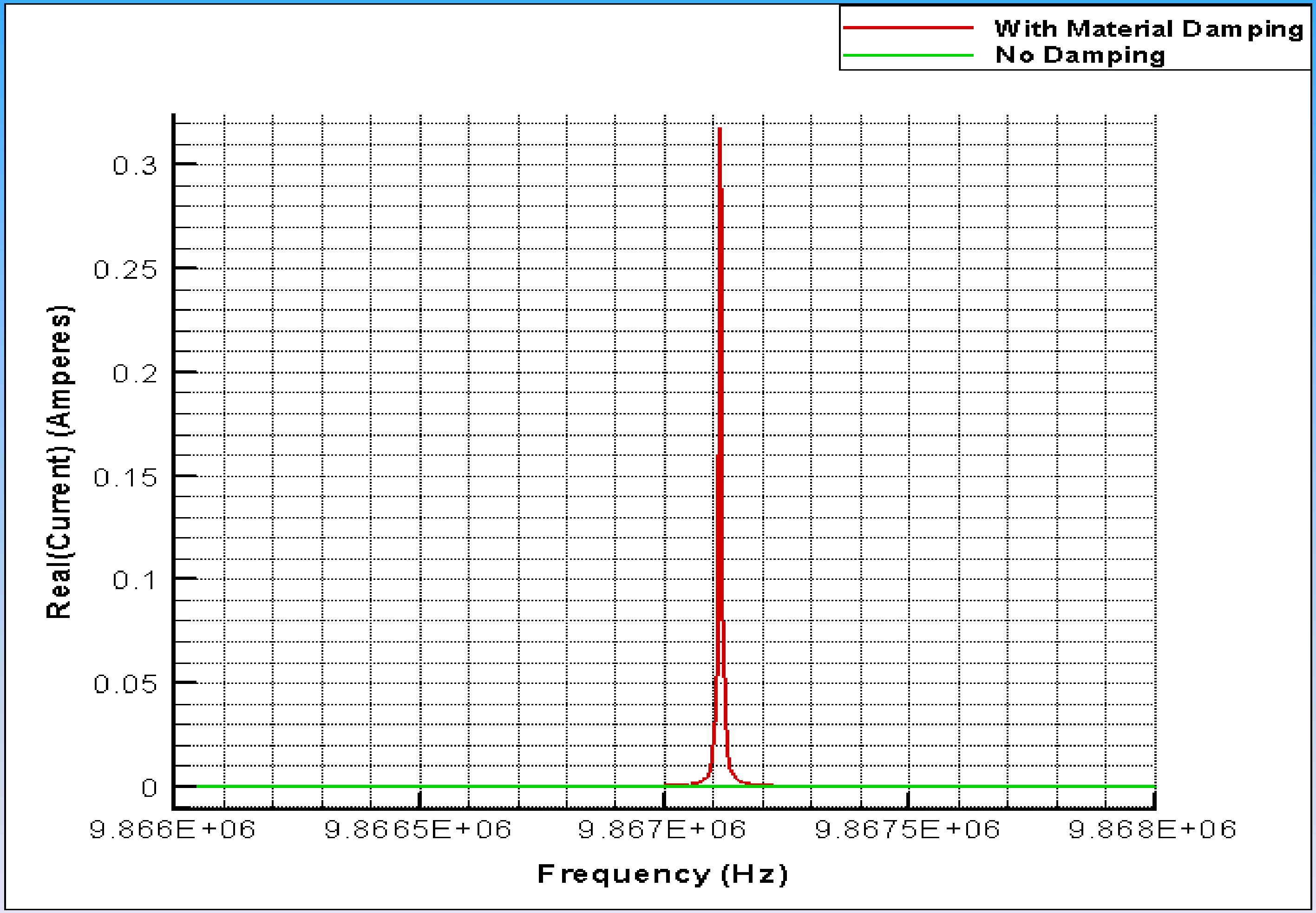

Real Part of current plot

Frequency response analysis for AT-cut quartz plate with and without dissipation

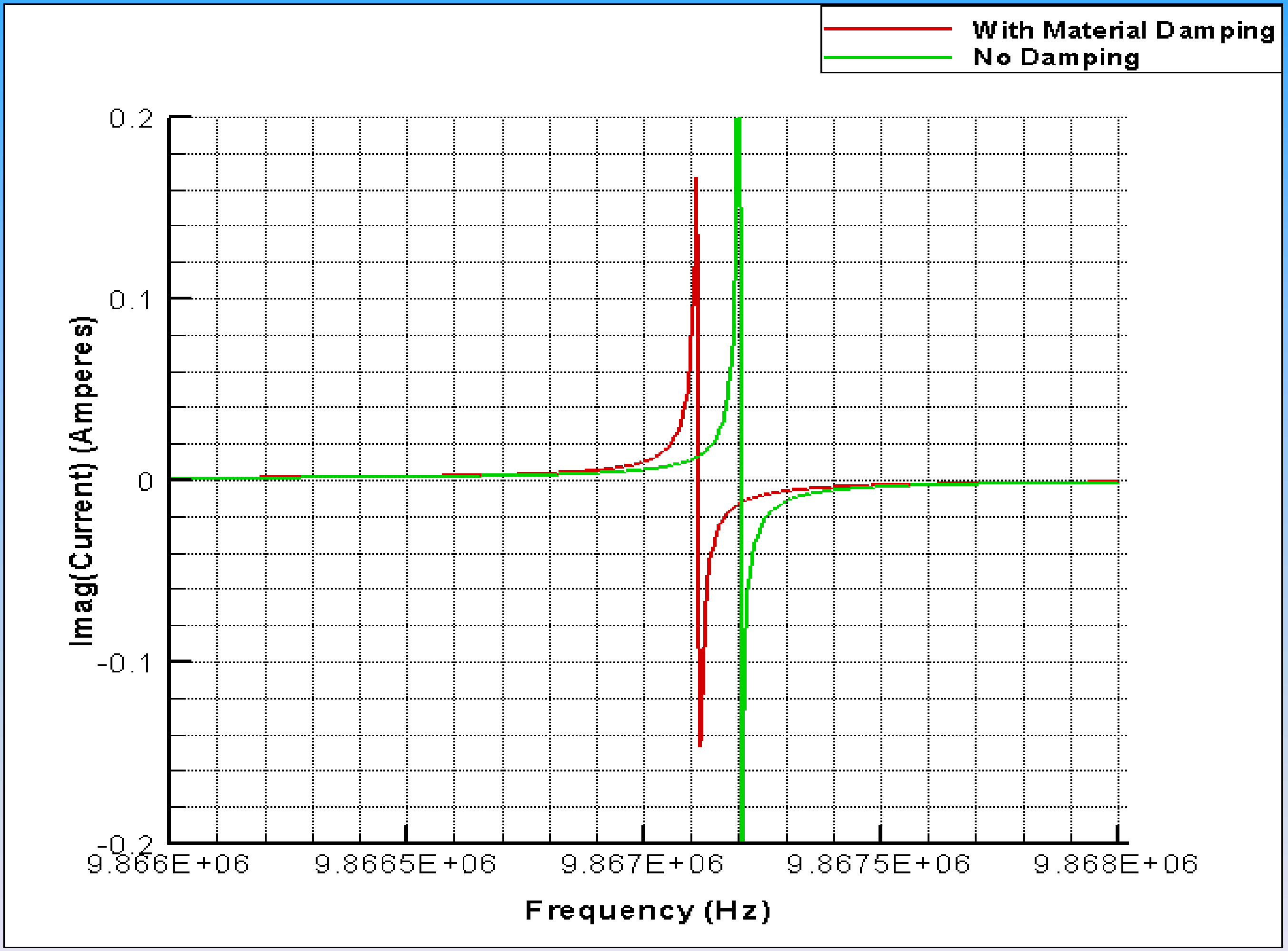

Imaginary part of current plot

Study of a tuning fork, and determination of its equivalent electrical parameters from the finite element model admittance curve (frequency response analysis)

Finite element model admittance curve $Y=G+jB$

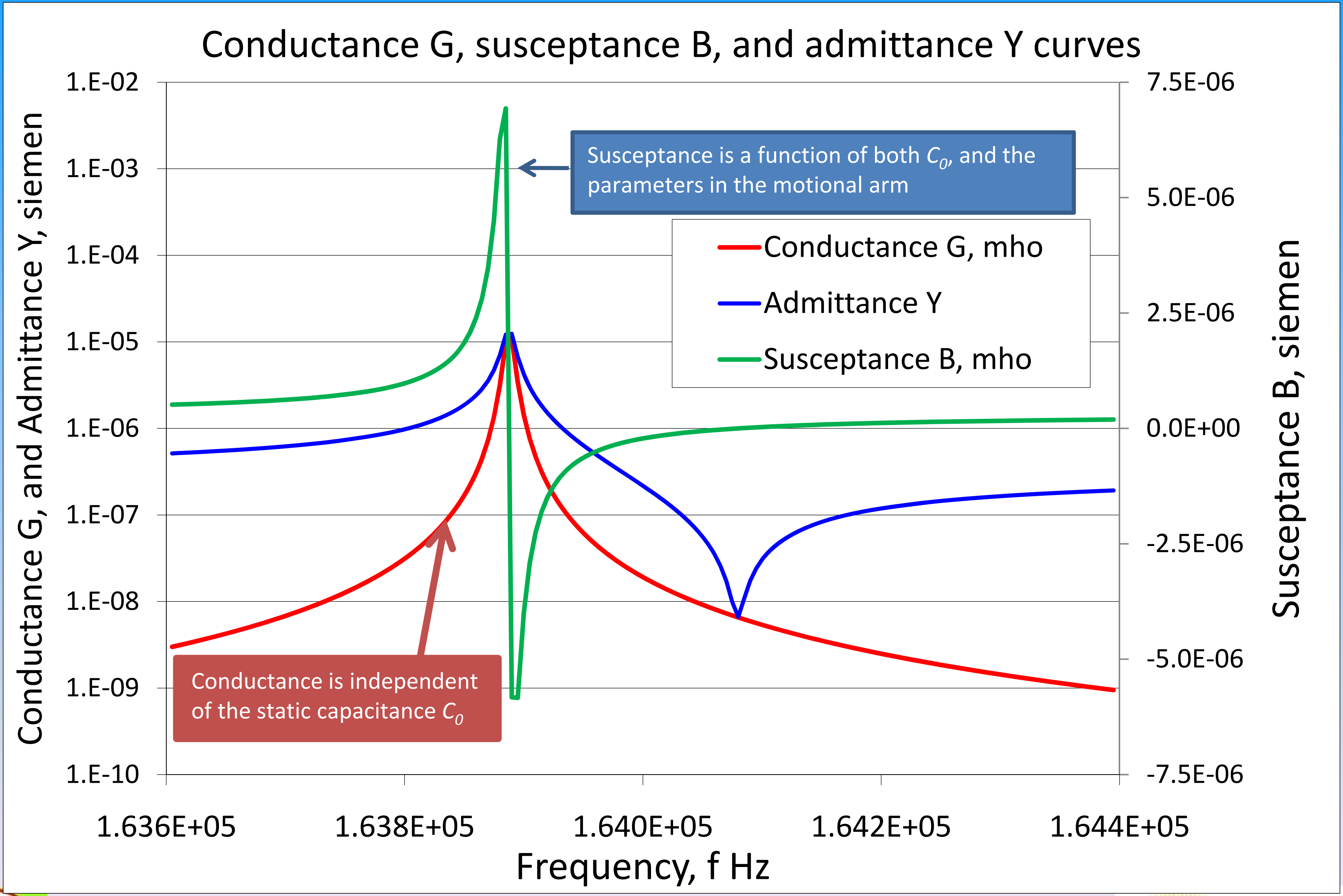

Steps for extracting the BVD model parameters

1. The static capacitance C_0 must be obtained first. One electrode is grounded, while the other electrode is applied with 1 V. The magnitude of the charge over the 1 V electrode is C_0 .

Steps for extracting the BVD model parameters

2. Determine the resistance and reactance of the motional arm
   a) Calculate $B_1 = B - \omega C_0$
   b) Calculate $R_1 = \dfrac{G}{G^2 + B_1^2}$
   c) Calculate $X_1 = -\dfrac{B_1}{G^2 + B_1^2}$
   d) Calculate $\dfrac{dX_1}{df}$ by the central difference method: $\left[\dfrac{dX_1}{df}\right]_i = \dfrac{[X_1]_{i+1} - [X_1]_{i-1}}{f_{i+1} - f_{i-1}}$

Steps for extracting the BVD model parameters

3. Note the series resonance f_s at the maximum admittance Y
4. Obtain the value of R_1 at $f = f_s$
5. Obtain the value of L_1 at $f = f_s$
6. Obtain the value of C_1 at $f = f_s$
7. Obtain the value of Q at $f = f_s$

Note:

$$L_1 = \frac{1}{4\pi}\frac{dX_1}{df}\bigg|_{f=f_s}$$

$$C_1 = \frac{1}{4\pi f_s^2 L_1}\bigg|_{f=f_s}$$

$$Q = \frac{1}{2\pi f_s C_1 R_1}\bigg|_{f=f_s}$$

Results for a 2° Z-cut 163 KHz quartz tuning fork resonator

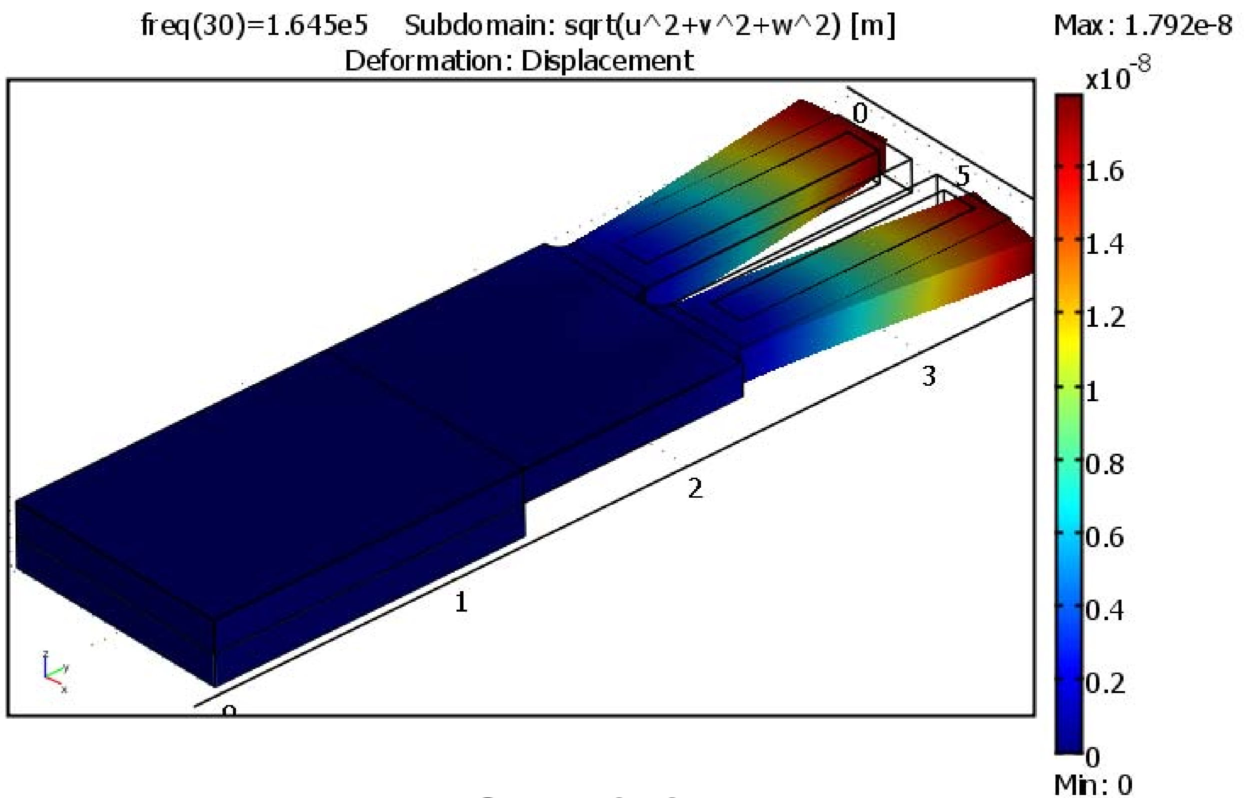

$C_0 = 0.3$ pF

Admittance curve of a tuning fork with base on a mounting support (no PML), 2° Z-cut quartz with Lamb & Richter damping. (Frequency range 140 KHz to 240KHz with a frequency increment of 200 Hz)

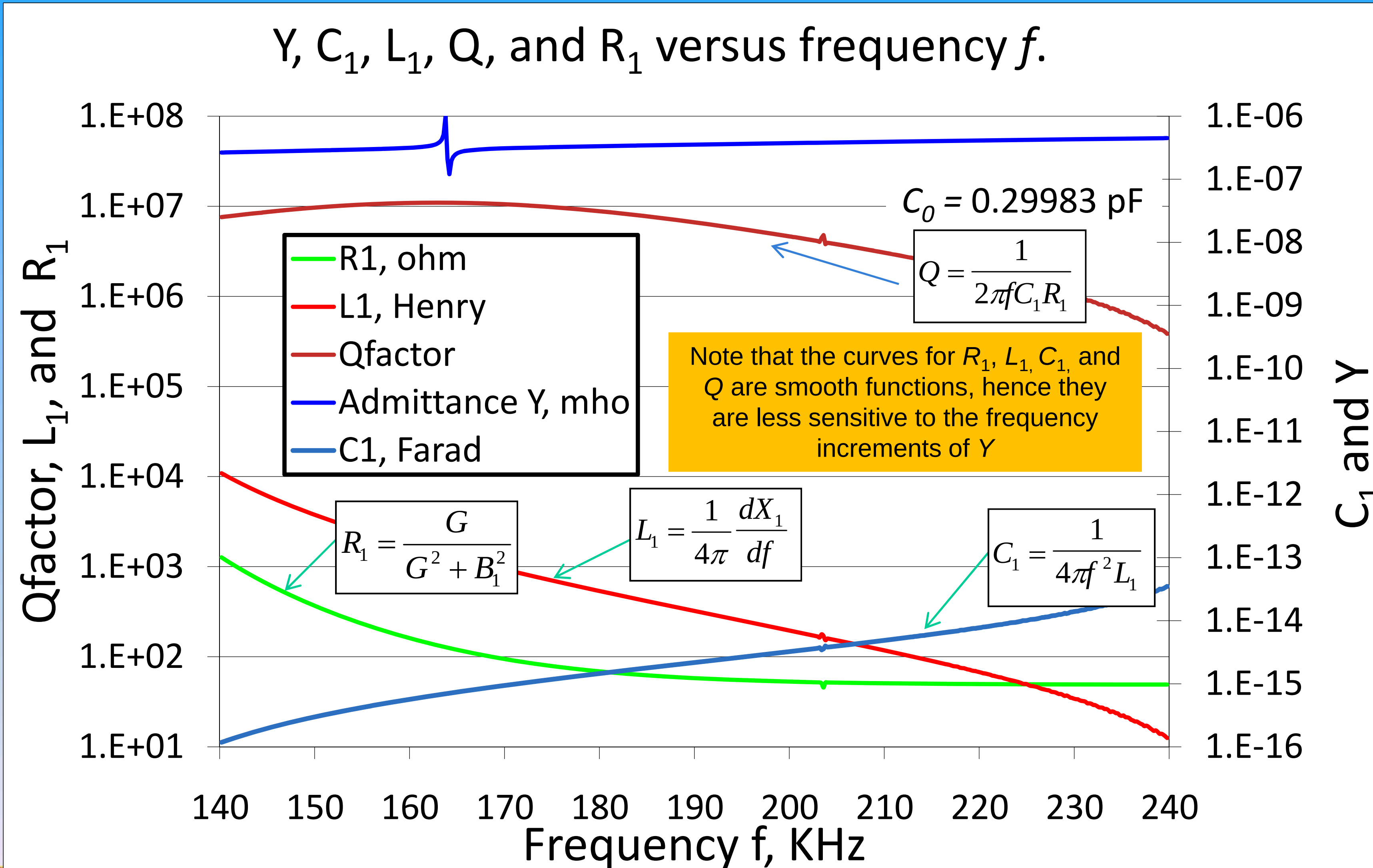

Admittance curve of a tuning fork with base on a mounting support (no PML), 2° Z-cut quartz with Lamb & Richter damping. (Frequency range 140 KHz to 240KHz with a frequency increment of 200 Hz)

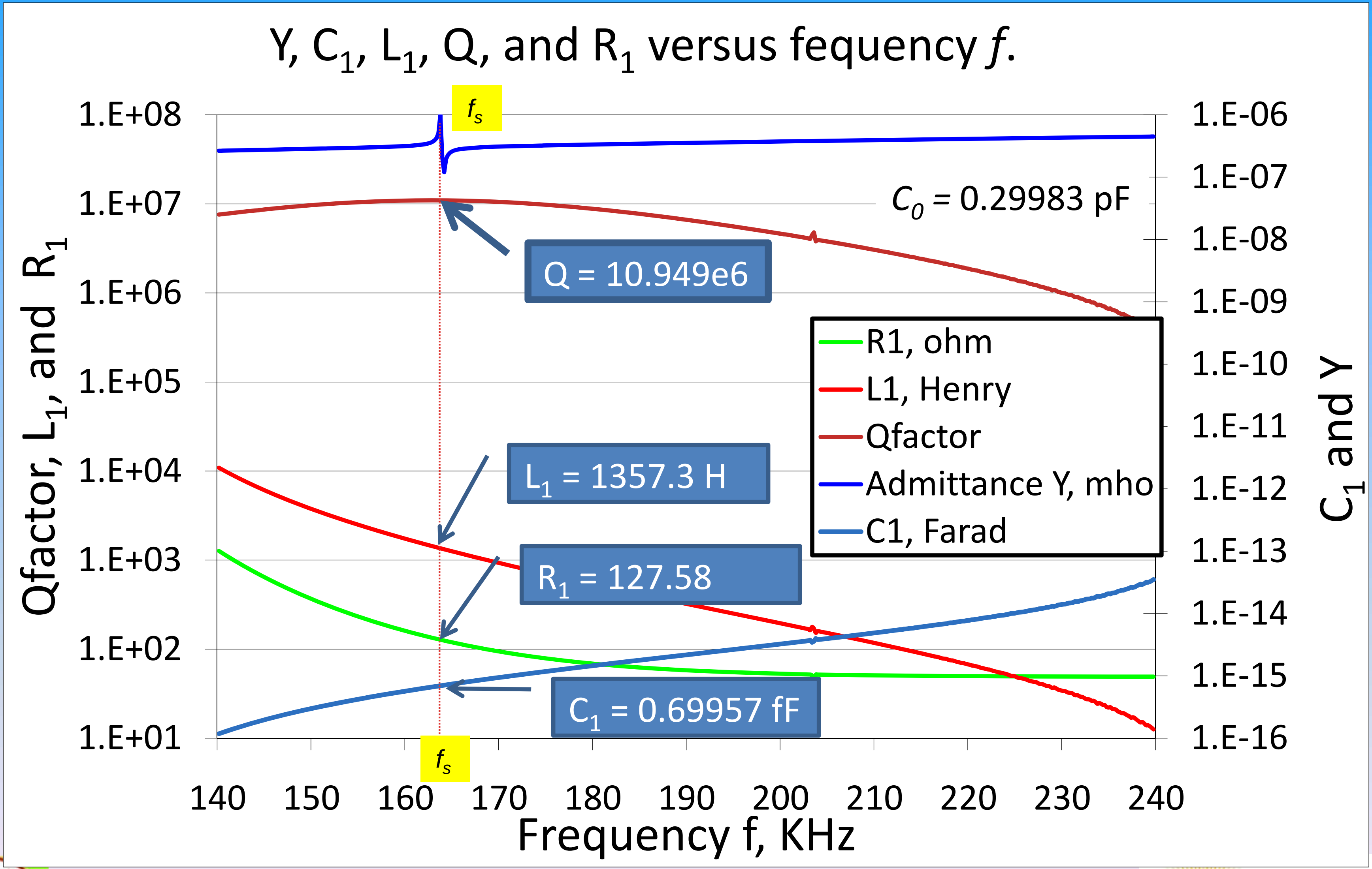

Comparison of the BVD electrical parameters obtained from the FEM admittance curves with different frequency increments

FEM admittance curve with frequency range 140 KHz to 240 KHz, and frequency increments of 200 Hz

C_0 = 0.29983 pF
R_1 = 127.58 ohm
L_1 = 1357.3 H
C_1 = 0.69957 fF
Q = 10.949x10^6

FEM admittance curve with frequency range 163.6 KHz to 164.4 KHz, and frequency increments of 5 Hz

C_0 = 0.29983 pF
R_1 = 126.12 ohm
L_1 = 1350.6 H
C_1 = 0.69830 fF
Q = 10.949x10^6

Comparison of admittance curves of a tuning fork with base on a mounting support (no PML), 2° Z-cut quartz with Lamb & Richter damping. (Frequency range 163.6 KHz to 164.4 KHz with a frequency increment of 5 Hz)

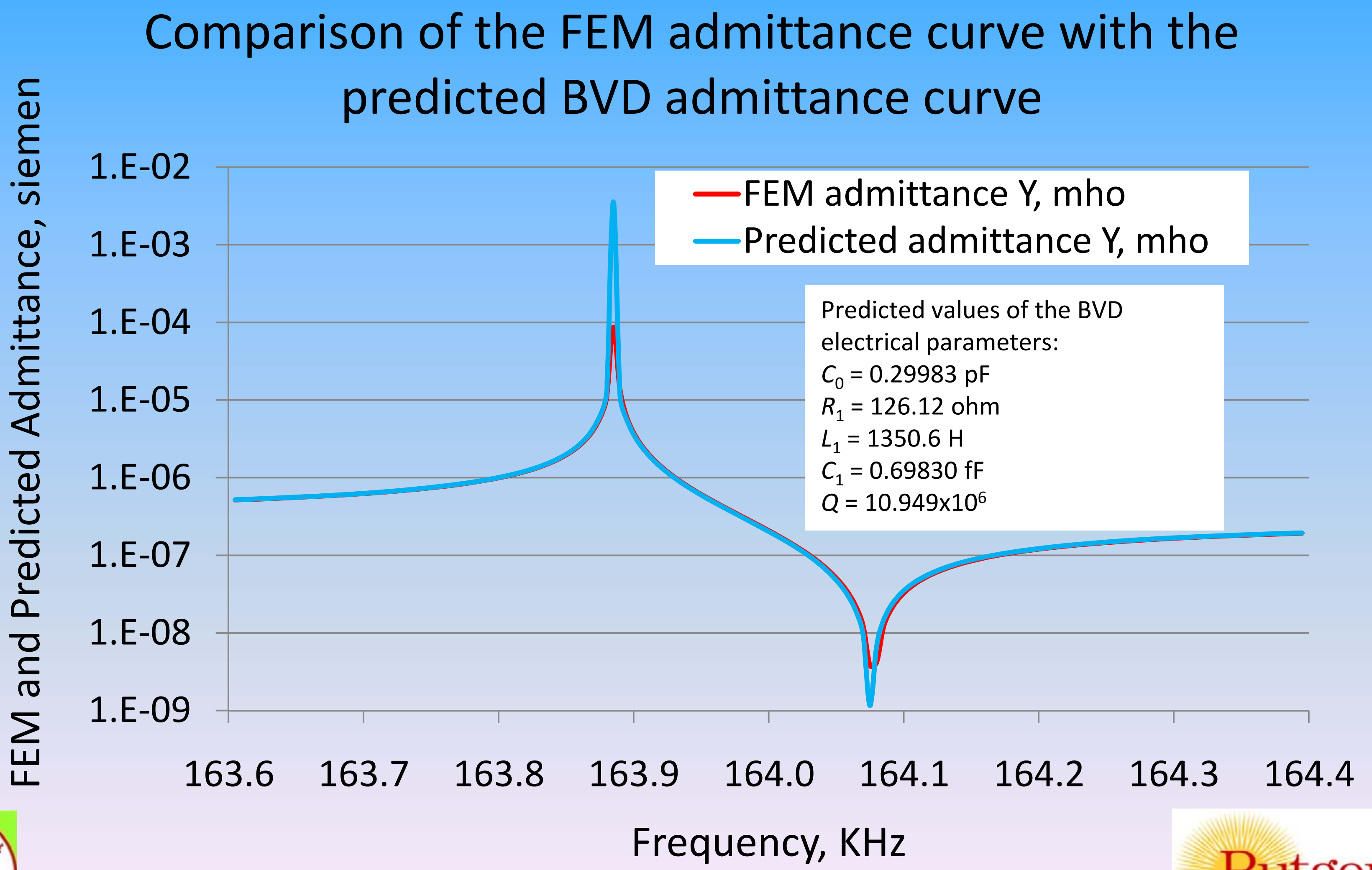

Effects of dissipation (PML) at the mounting supports on the BVD model parameters

Admittance curve of a tuning fork with base fixed on a mounting support (with PML), 2° Z-cut quartz with Lamb & Richter damping. (Frequency range 163.6 KHz to 164.4 KHz with a frequency increment of 5 Hz)

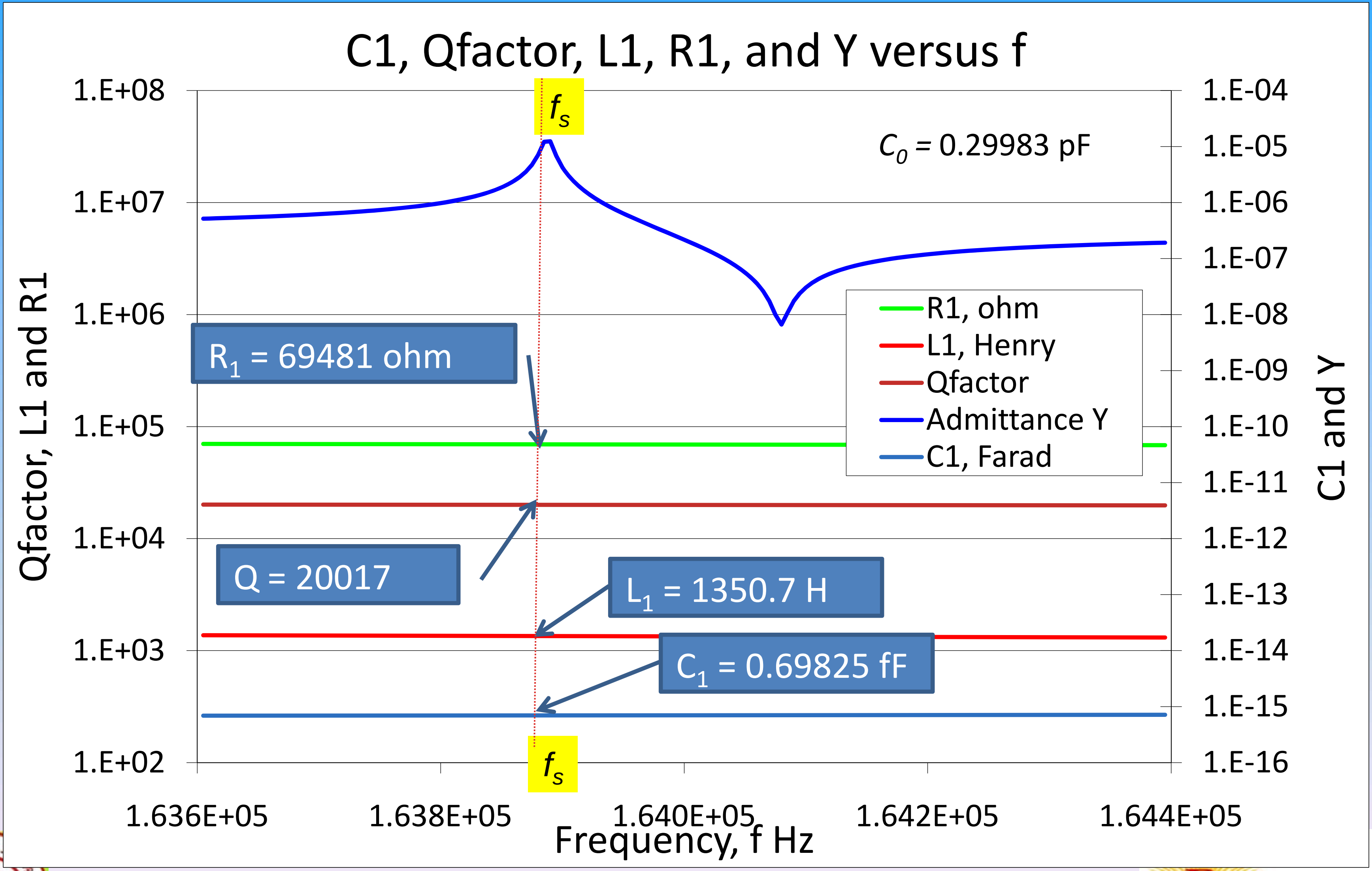

Comparison of the effects of dissipation (PML) at the mounting support on the BVD electrical parameters

No PML at the mounting support

FEM admittance curve with frequency range 163.6 KHz to 164.4 KHz, and frequency increments of 5 Hz

C_0 = 0.29983 pF
R_1 = 126.12 ohm
L_1 = 1350.6 H
C_1 = 0.69830 fF
$Q = 10.949 \times 10^6$

With PML at the mounting support

FEM admittance curve with frequency range 163.6 KHz to 164.4 KHz, and frequency increments of 5 Hz

C_0 = 0.29983 pF
R_1 = 69481 ohm
L_1 = 1350.7 H
C_1 = 0.69825 fF
Q = 20017

Frequency response before mounting onto a base in the package

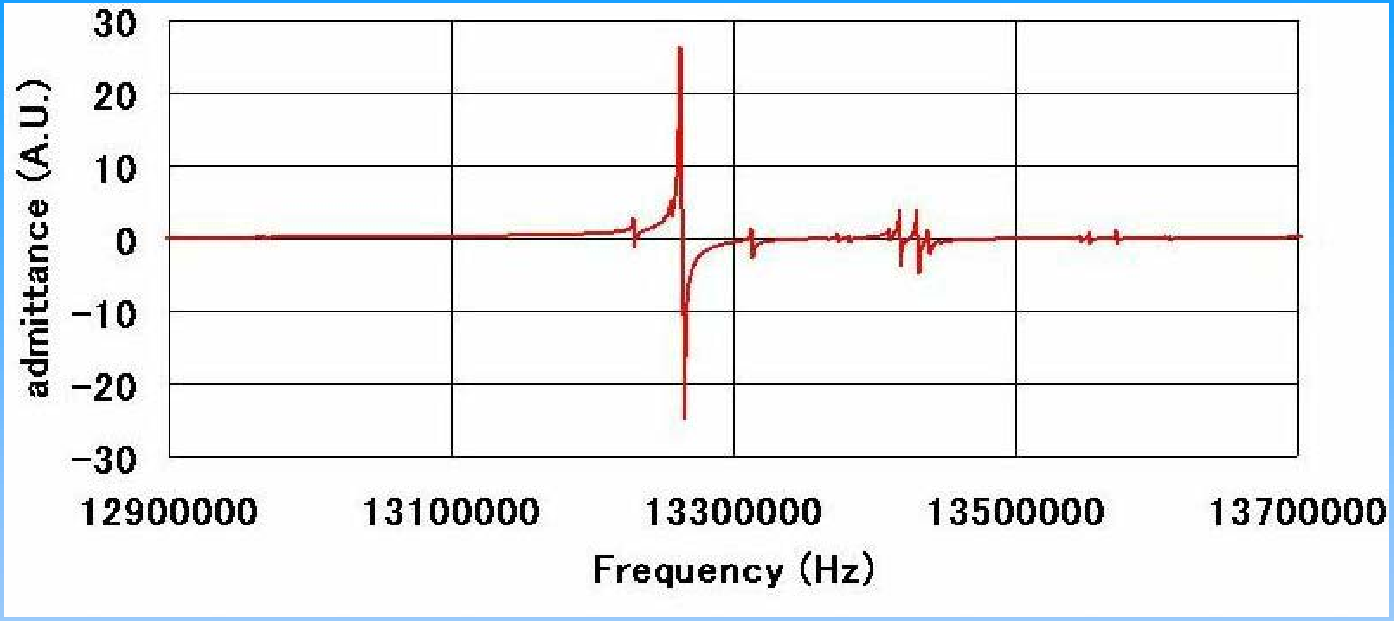

Frequency response after mounting onto a base in the package

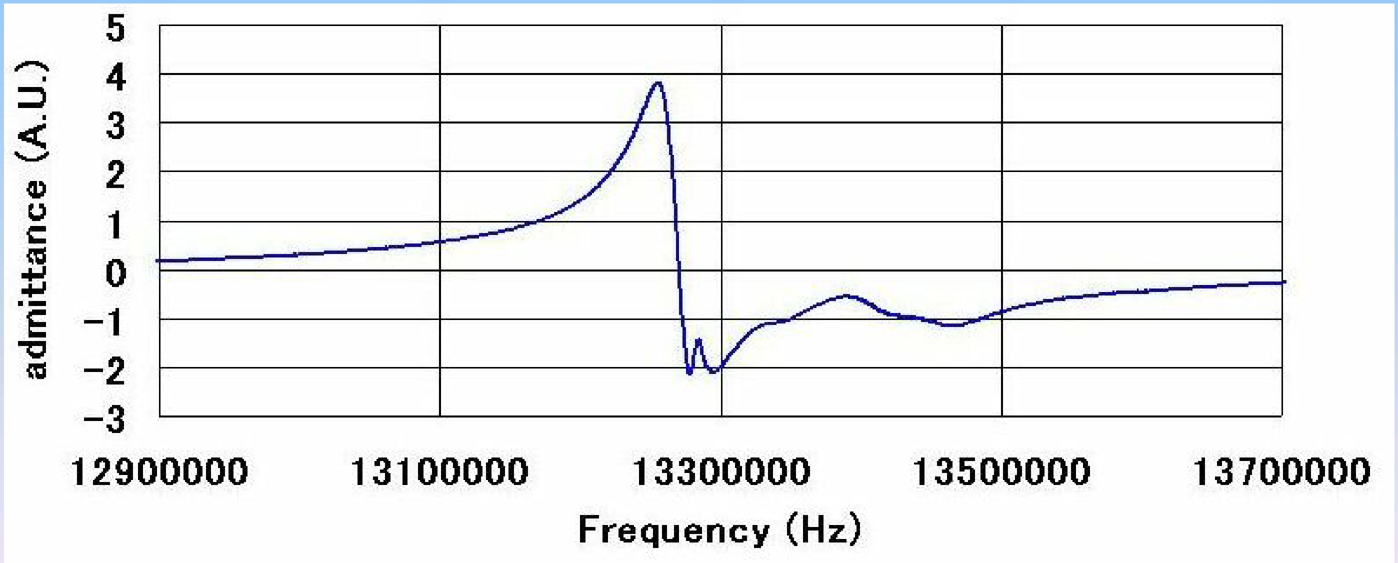

The effects of packaging

Frequency response before packaging

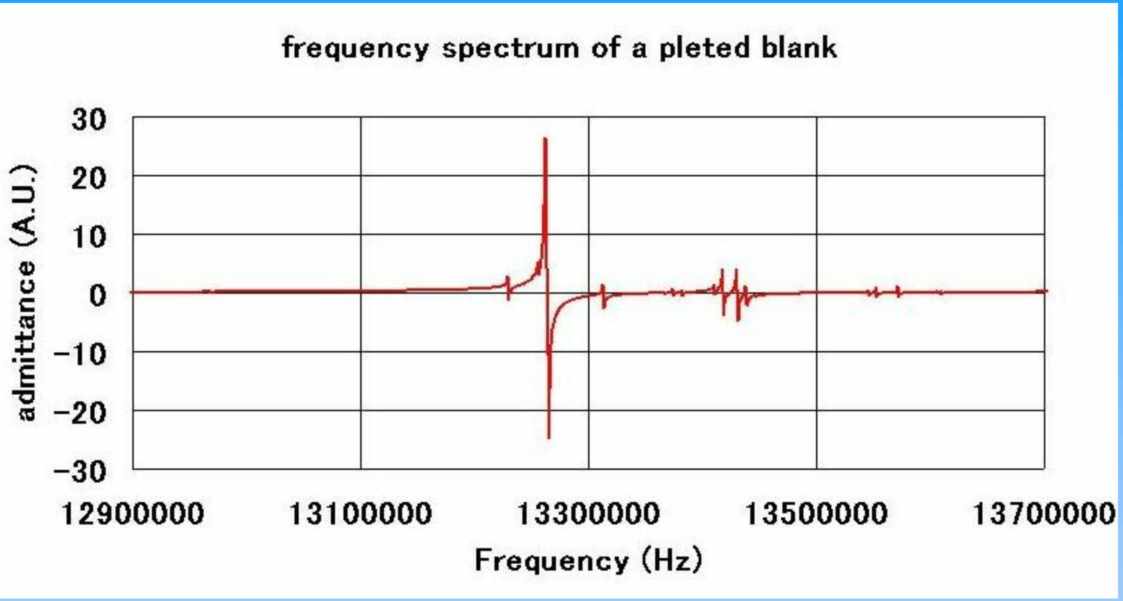

Frequency response after packaging

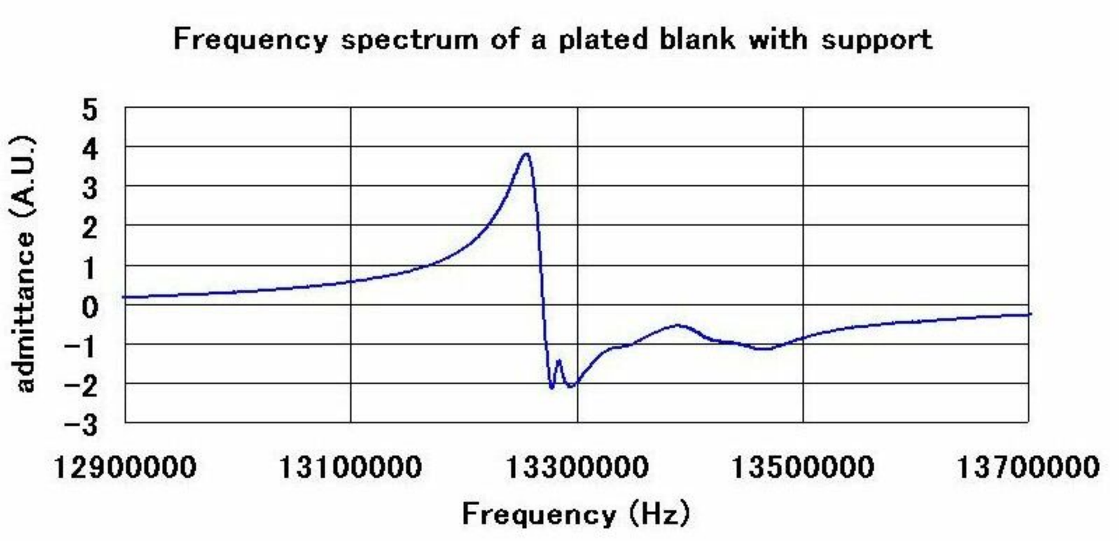

FEM model with an energy sink

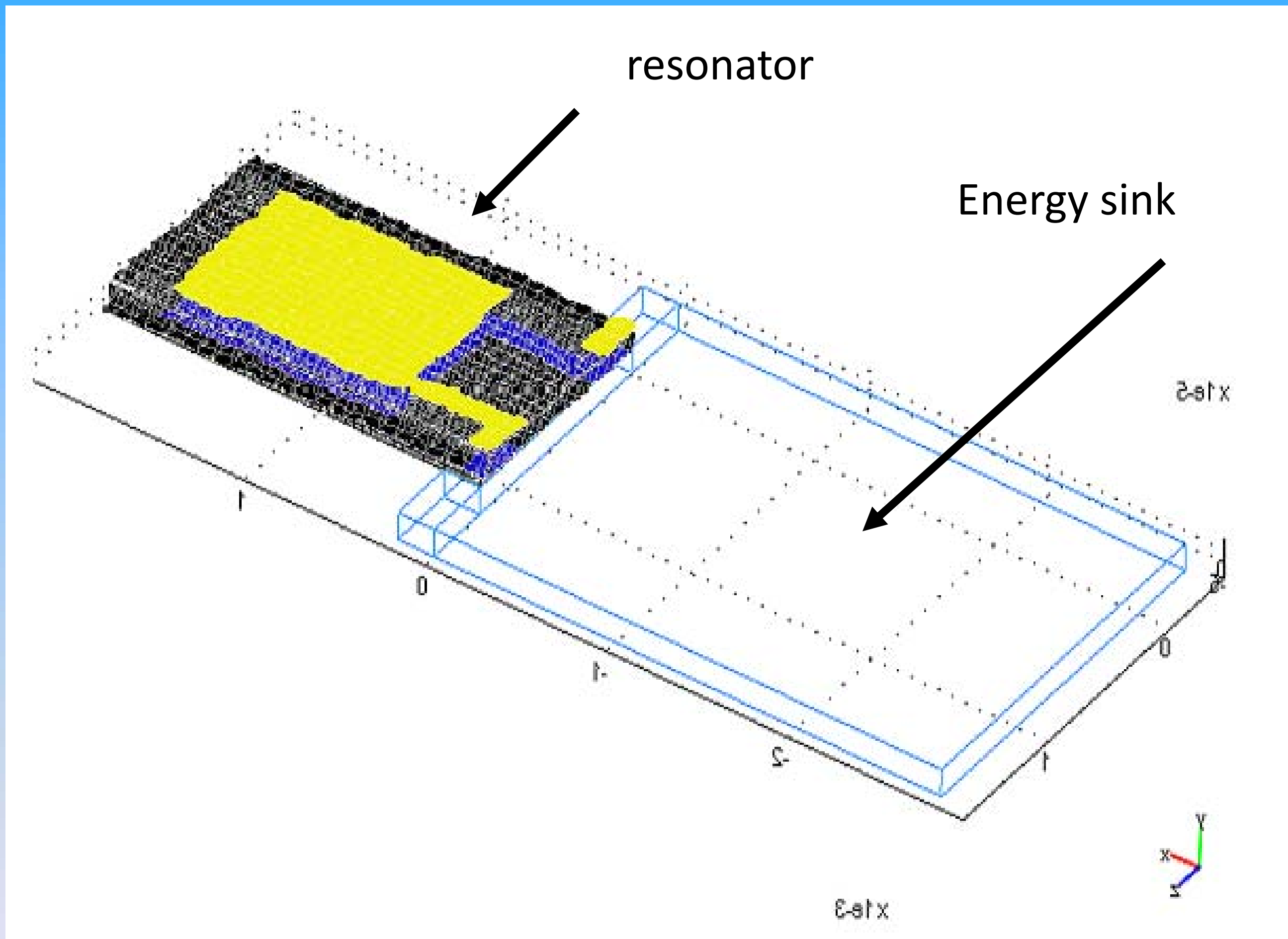

Two types of energy absorbing base could be modeled

- Base with acoustic loss as an energy sink

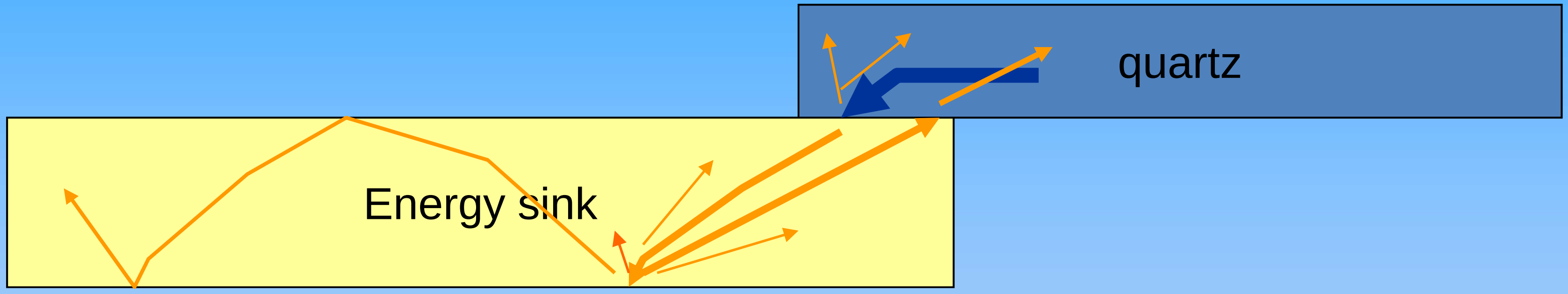

- Perfectly Matched Layer as an energy sink

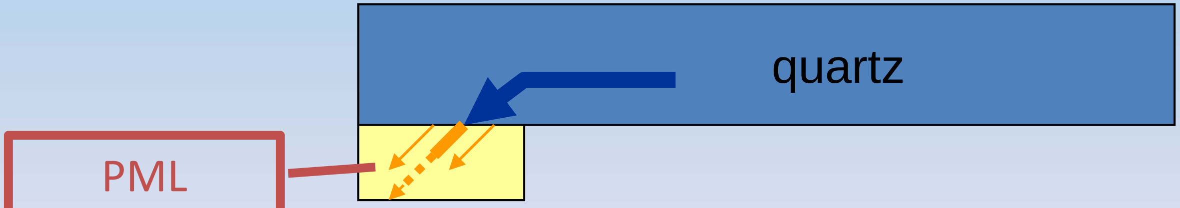

No reflection at the interface
Perfect decay of the wave at bottom layer

13 MHz case

48 MHz case

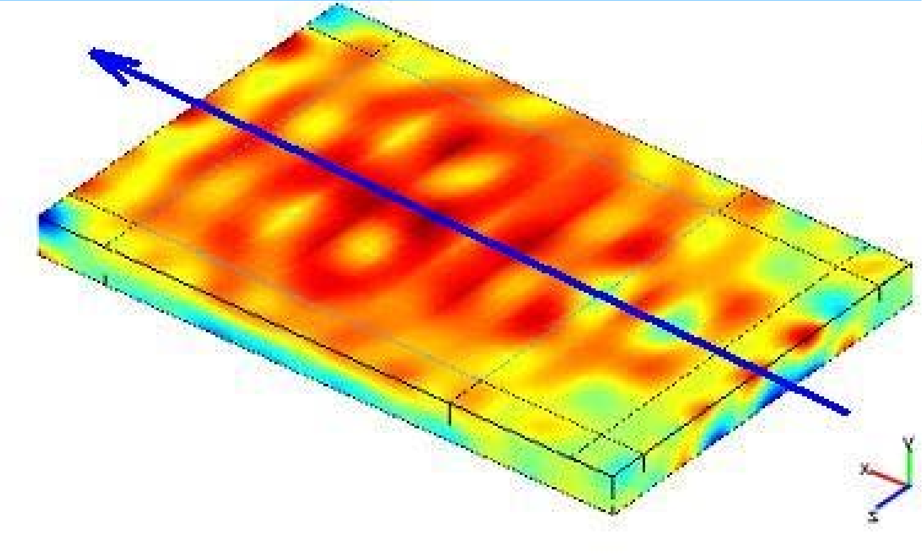

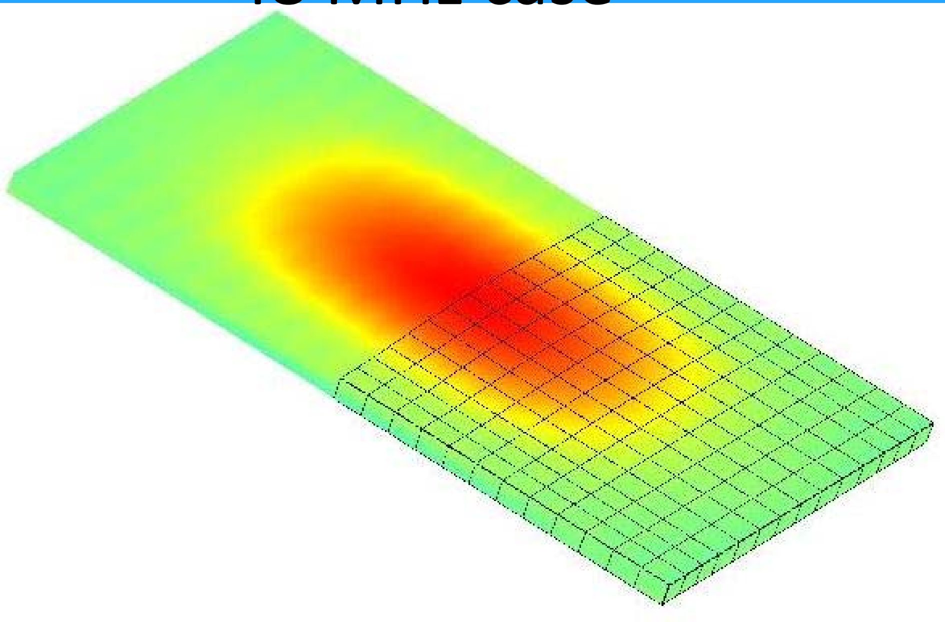

Energy trapping not good, large acoustic energy losses to the base

Good energy trapping, minimal acoustic energy losses to the base

Frequency response analysis (13 MHz case)

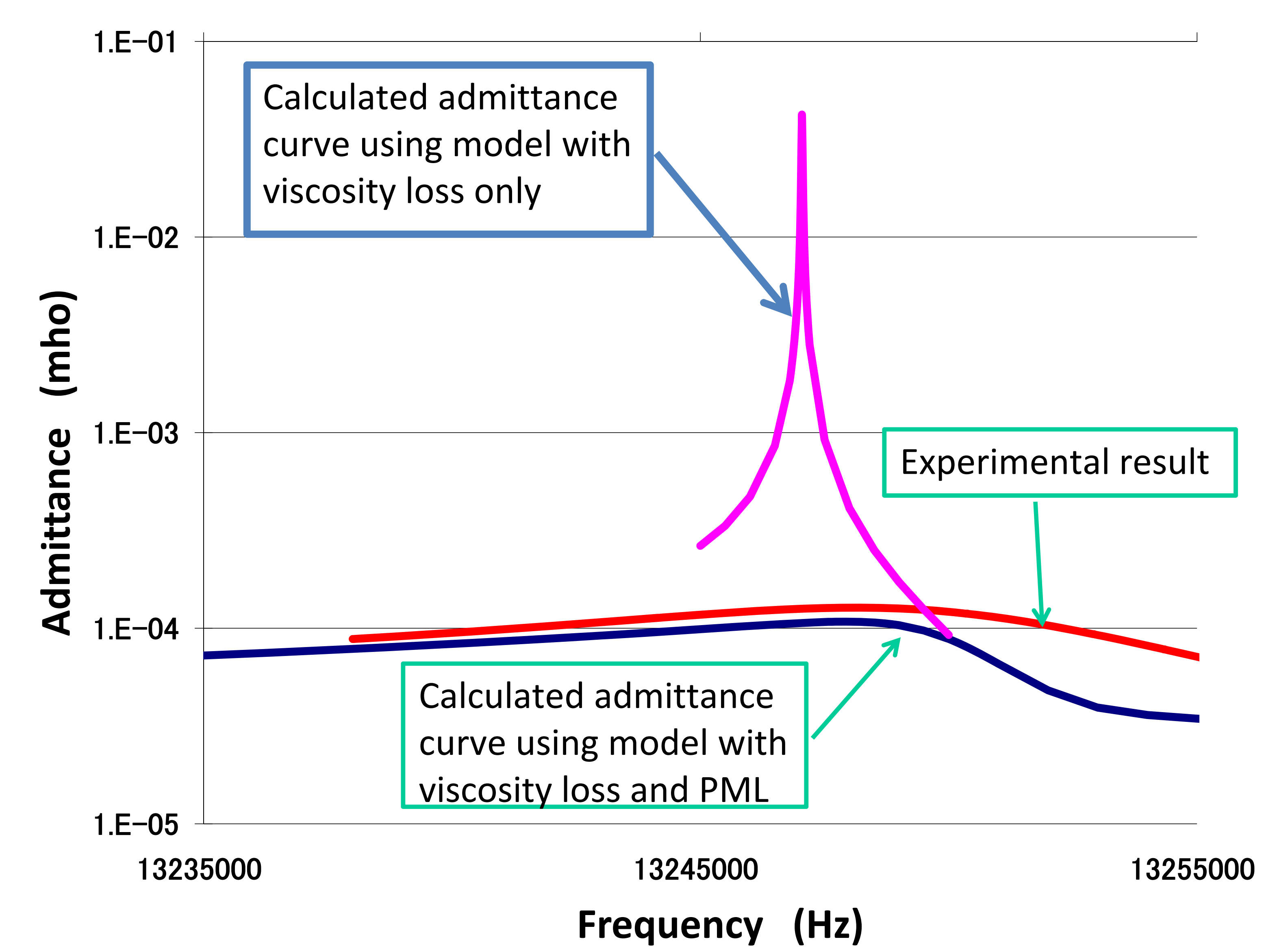

Frequency response analysis (48 MHz case)

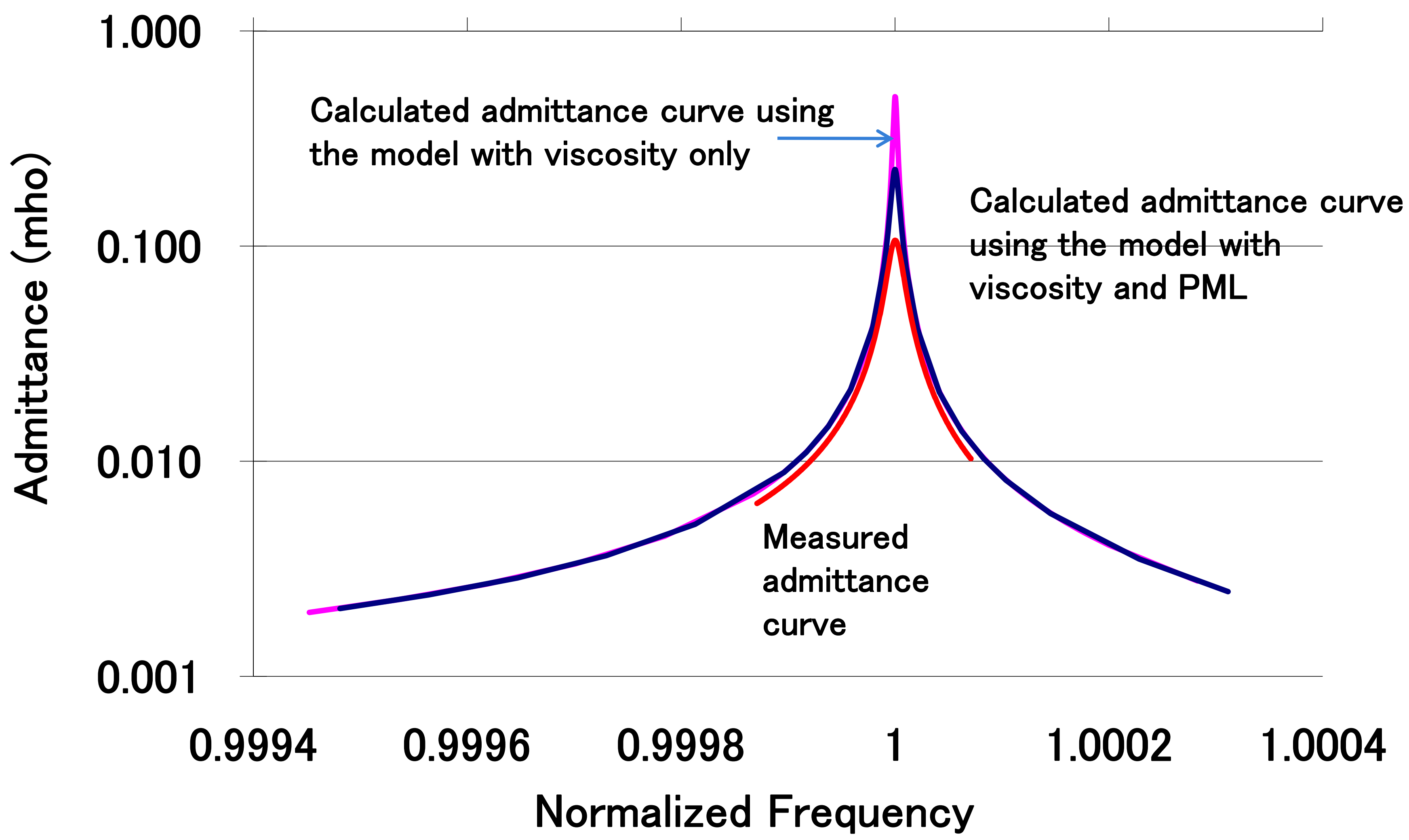

Comparison of calculation results with experimental results

13MHz Atcut resonator

sample	F r(MHz)	Q factor	R1(ohm)
experiment	13.253	1067	10730
with PML with viscosity	13.247	982	9256
without PML with viscosity	13.247	630000	24
Fix condition at support	13.271	1000000	8.5

48MHz ATcut resonator

sample	F r(MHz)	Q factor	R1(ohm)
experiment	47.997	69110	9.41
with PML with viscosity	48.165	199423	4.40
with PML, viscosity, lead resistanc	48.165	175492	5.00
without PML with viscosity	48.166	427159	2.03

Q factor can be estimated by consideration of both viscosity loss and supporting loss.

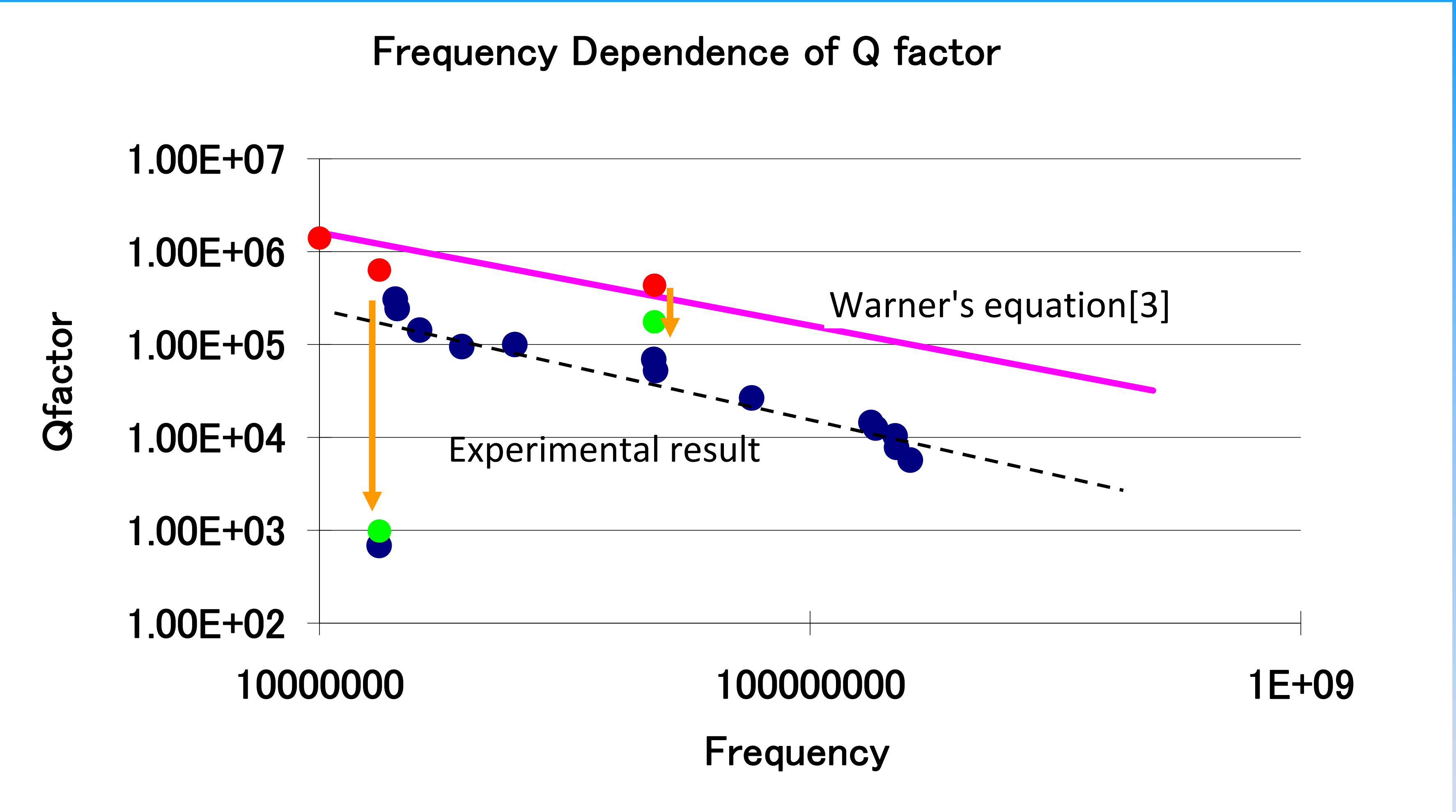

- Q factors with viscosity loss
- Q factor with viscosity + PML

[3] A. W. Warner, "Design and Performance of Ultraprecise 2.5-mc Quartz Crystal Units," The Bell System Technical Journal, pp. 1193-1217, September 1960

Analytical Considerations

There are no closed form analytical solutions for a 3-D resonator with finite dimensions

Numerical methods are needed for designs

Finite Element Method

Validation of the finite element method:

a) The AT-cut fundamental thickness shear mode
b) Frequency spectrum and comparison with Koga’s experimental data
c) Frequency-temperature characteristics and comparison with Sekimoto, et. al.’s experimental data

The AT-cut fundamental thickness shear mode

- Mode shape
- High current at the plate surfaces

Finite element model of a 1 MHz AT-cut quartz plate

- Cut angle 35.25 degrees about the digonal axis
- Dimensions: 16 mm X-length, 27 mm Z-length, 1.65 mm thickness
- Lagrange quadratic hexahedral elements used
- 3 x 35 x 50-element mesh
- 30 eigenfrequencies calculated centered about 1 MHz

Finite element mesh

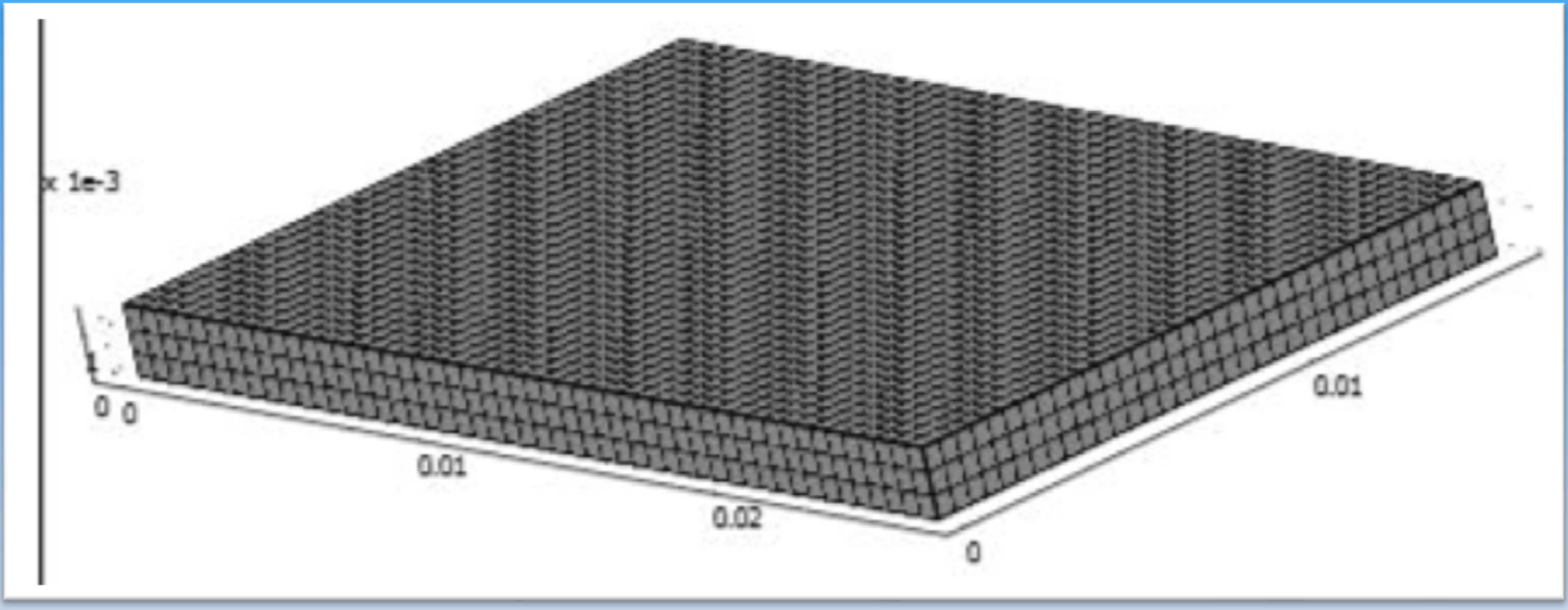

Thickness shear mode shape

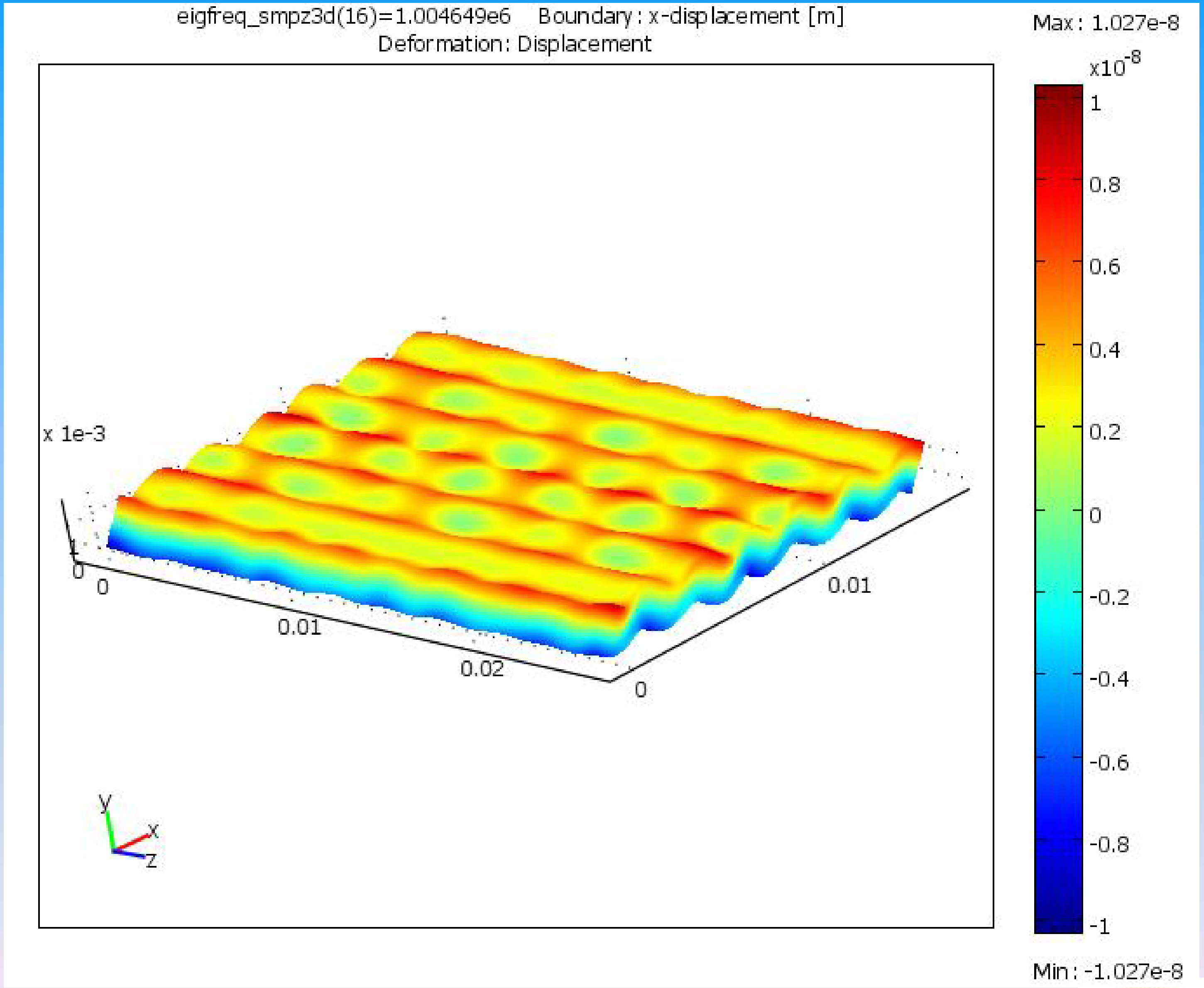

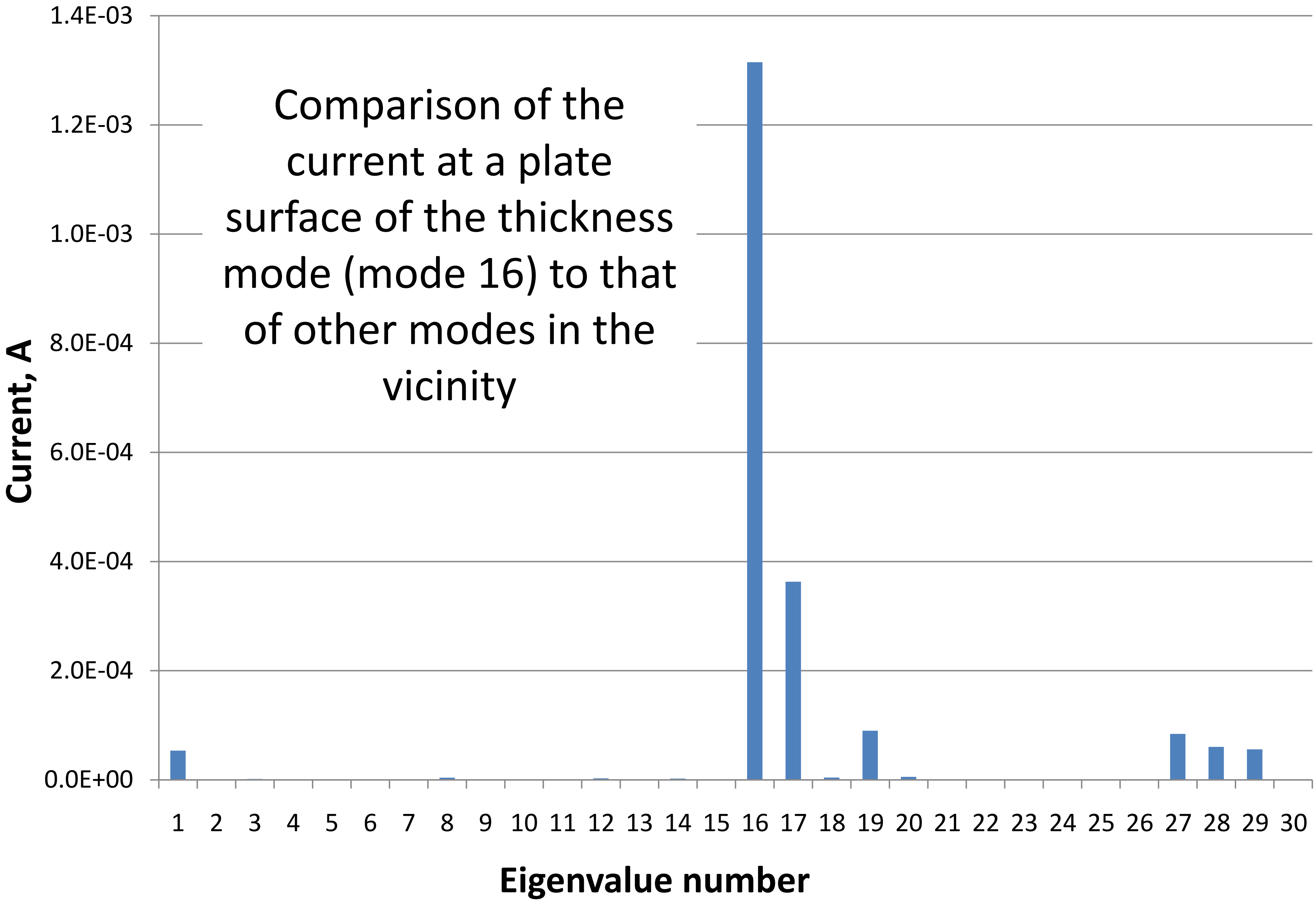
Comparison of the current at a plate surface of the thickness mode (mode 16) to that of other modes in the vicinity
Current, A
1.4E-03
1.2E-03
1.0E-03
8.0E-04
6.0E-04
4.0E-04
2.0E-04
0.0E+00
1 2 3 4 5 6 7 8 9 10 11 12 13 14 15 16 17 18 19 20 21 22 23 24 25 26 27 28 29 30
Eigenvalue number

Frequency spectrum and comparison with Koga's experimental data[1]

- Frequency spectrum = plot of resonant frequencies versus a parameter such as the length to thickness ratio (a/b)

[1] "Radio-Frequency Vibrations of Rectangular AT-cut Quartz Plates", Isaac Koga, Journal of Applied Physics, Vol. 34, No. 8, August 1963, pp 2357-2365

Koga's [1] frequency spectrum

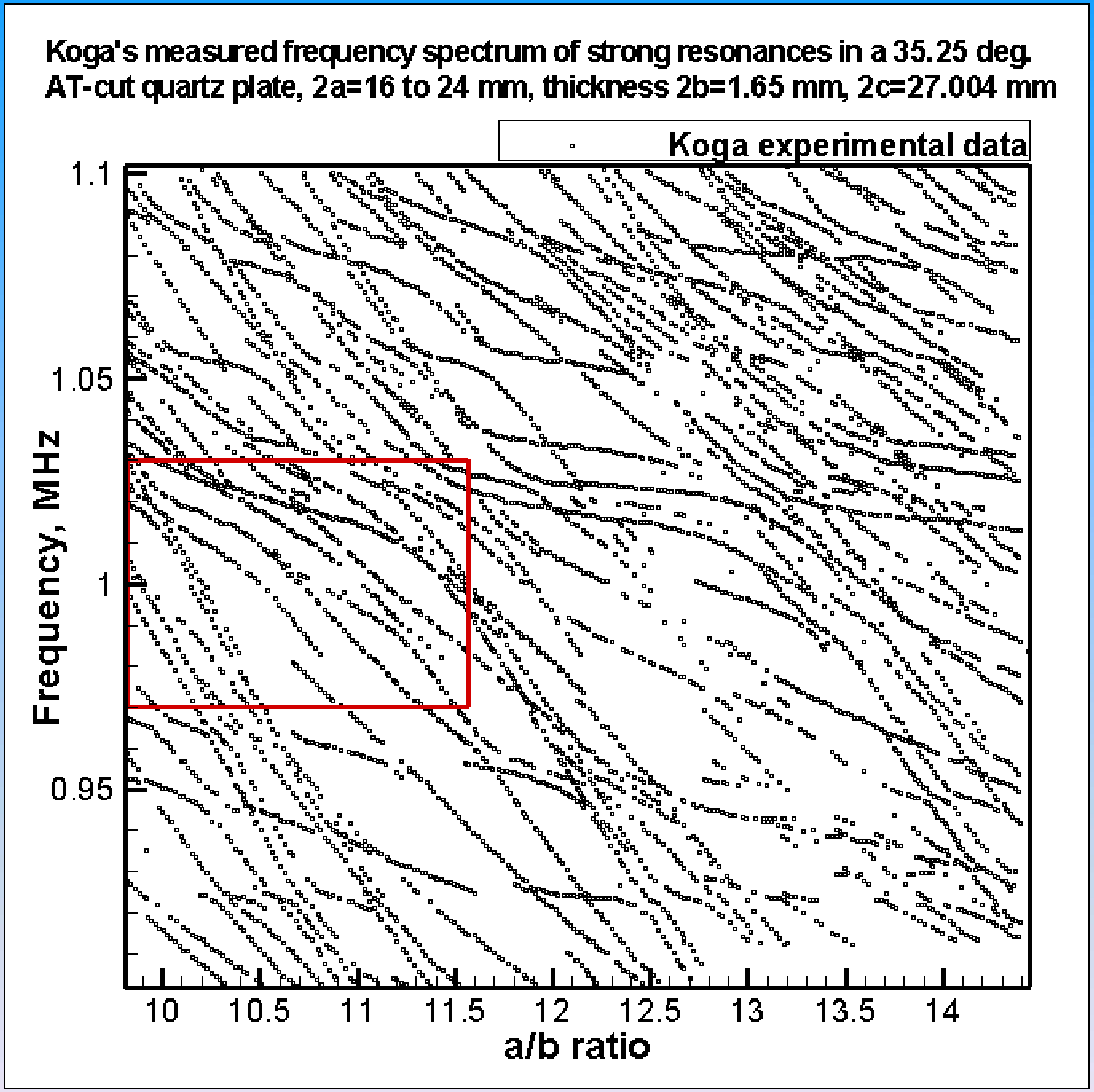

Notes:

1. Koga measured the strong resonances in a quartz plate as a function of the X-length from 16 mm to 24 mm
2. By meticulously "shaving" the X-length from 24 mm down to 16 mm, and carefully measuring and recording the strong resonances after each "shave", he produced the frequency spectrum on the left.
3. He used a pair of air-gap electrodes to drive the plate.
4. It is more meaningful to plot resonance frequencies against the dimensionless length a/b ratio.
5. The red rectangle on the graph delineates the range of values to be compared with COMSOL model results.

Sorting the COMSOL model results

- The modal frequencies were calculated along with their relative ratio of shear (xy) strain energy to total strain energy and current.
- The modes were sorted into three groups:

1. High ratio of shear (xy) strain energy to total strain energy and current modes
2. High current modes (this represent the strong resonant modes measured by Koga [1]
3. Other modes

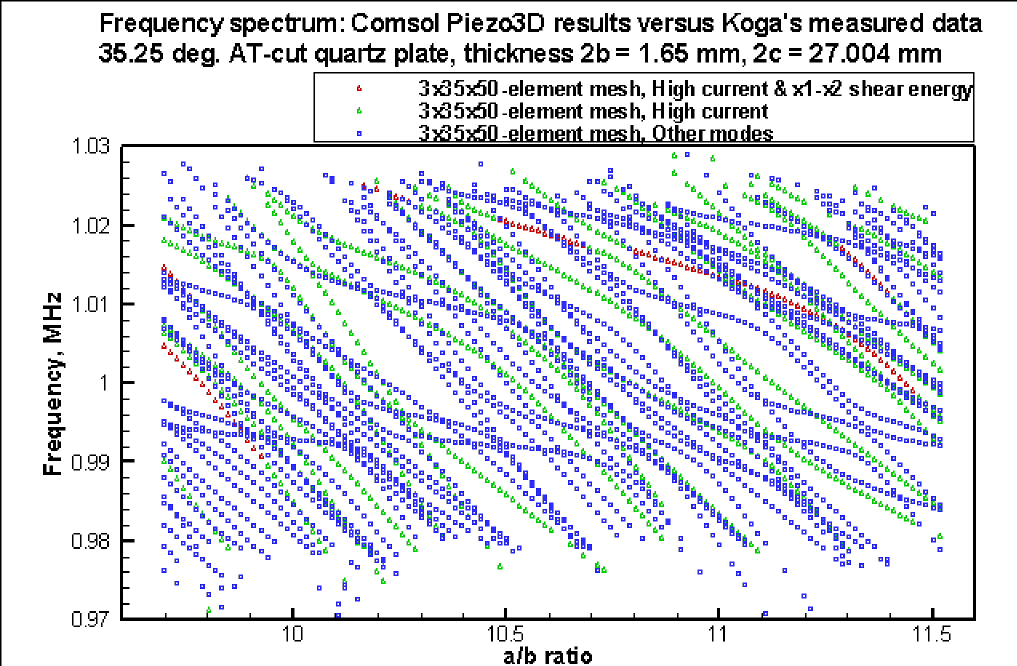

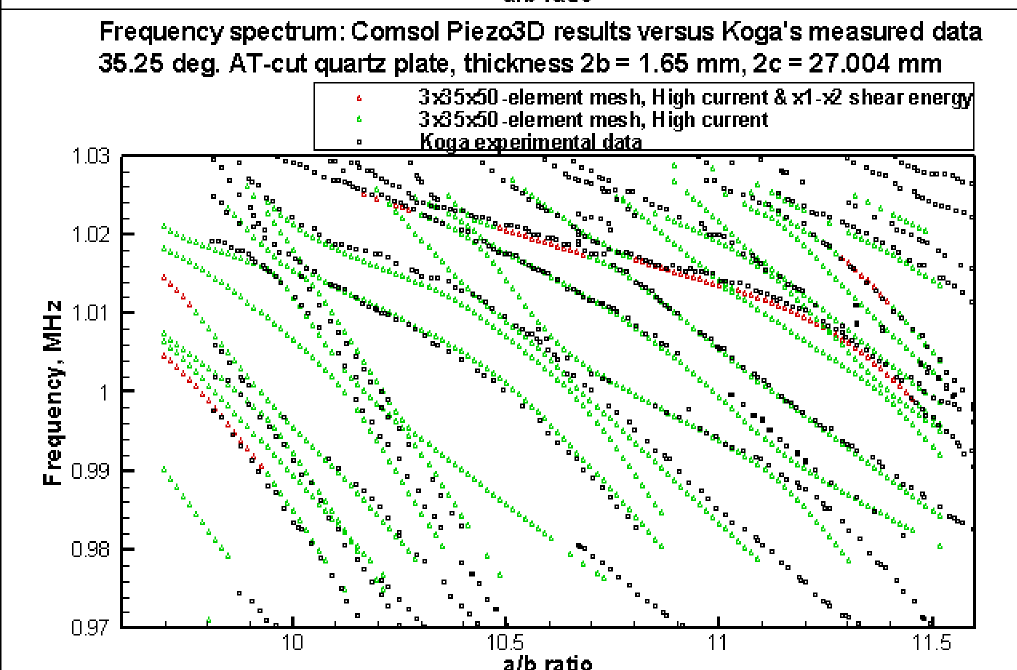

Notes:

1. The COMSOL model produced more modes than measured by Koga.
2. All the COMSOL model modes are real but most are too faint to be detected by a pair of air-gap electrodes.
3. There are charge cancellations in most of the modes hence they could not be driven by a pair of electrodes on the plate major surfaces.
4. The red modal branch represents modes which are strong in current and ratio of shear (xy) strain energy to total energy, and it is usually the thickness shear modal branch.
5. The green modal branch represents the modes which are strong in current, and it is usually the strong resonances measured by Koga.
6. The blue modal branch represents the other modes which are usually not detected by Koga. These modes are usually not driven in a quartz plate resonator, however they are the spurious modes that could cause problems due to unsymmetrical electrodes& plate, mounting supports, nonlinear behavior, etc.

Frequency-temperature characteristics and comparison with Sekimoto, et. al.'s experimental data[2]

- Frequency deviations versus temperature

[2] H. Sekimoto, S. Goka, A. Ishizaki, and Y. Watanabe, "Frequency-temperature behavior of spurious vibrations of rectangular AT-quartz plates," Proceedings of the 1997 IEEE International Frequency Control Symposium, pp. 710-714, 1997

Finite element model of a 0.96 MHz AT-cut quartz plate

- Cut angle 35.25 degrees about the digonal axis
- Dimensions: 13.964 mm X-length, 7.000 mm Z-length, 1.737 mm thickness
- Lagrange quadratic tetrahedral elements used
- Mesh generated using free meshing of maximum element size 0.8 mm.
- 20 eigenfrequencies calculated about the 0.96 MHz

Thickness shear mode shape

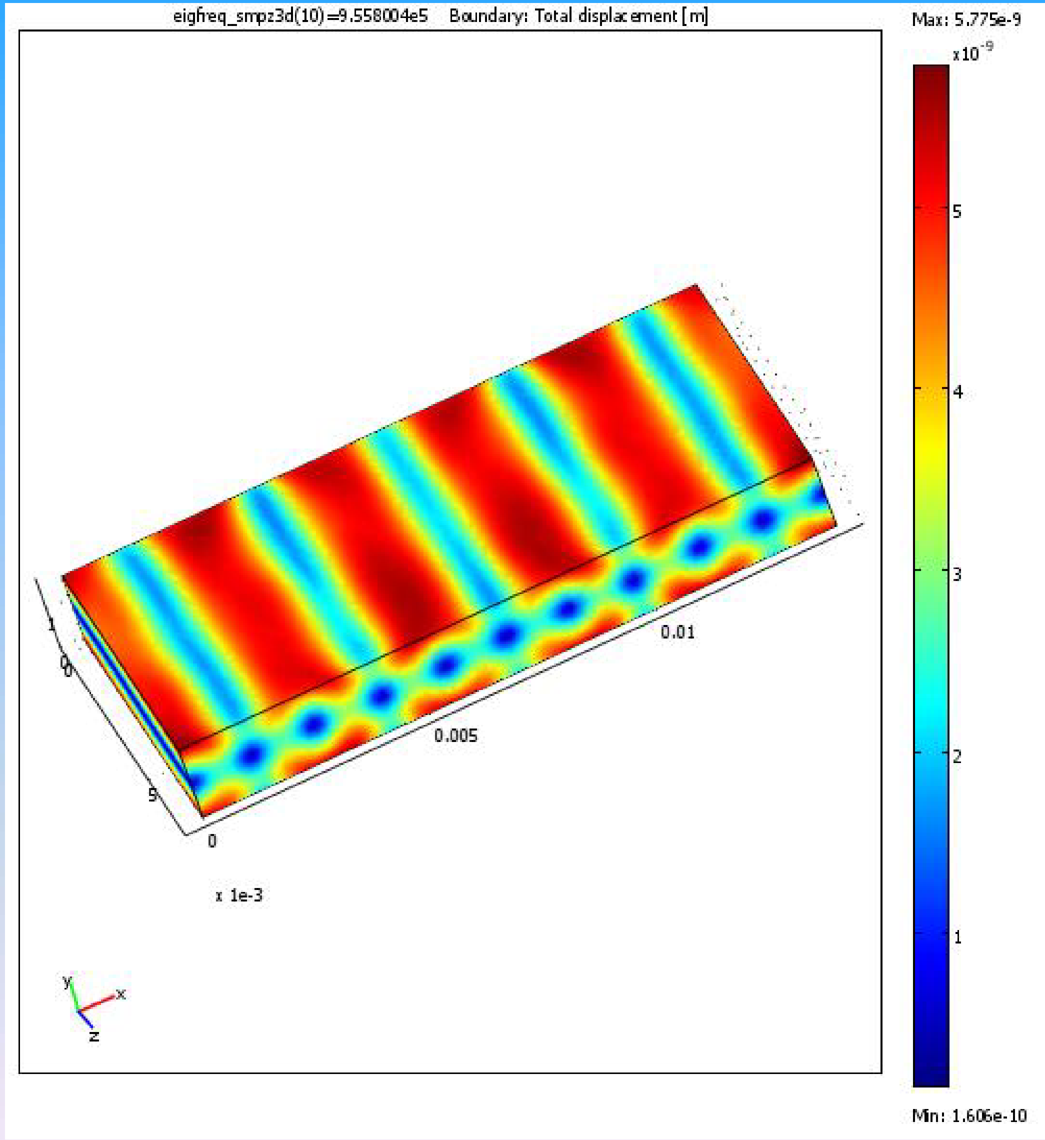

Strong resonances (high current) as a function of temperature

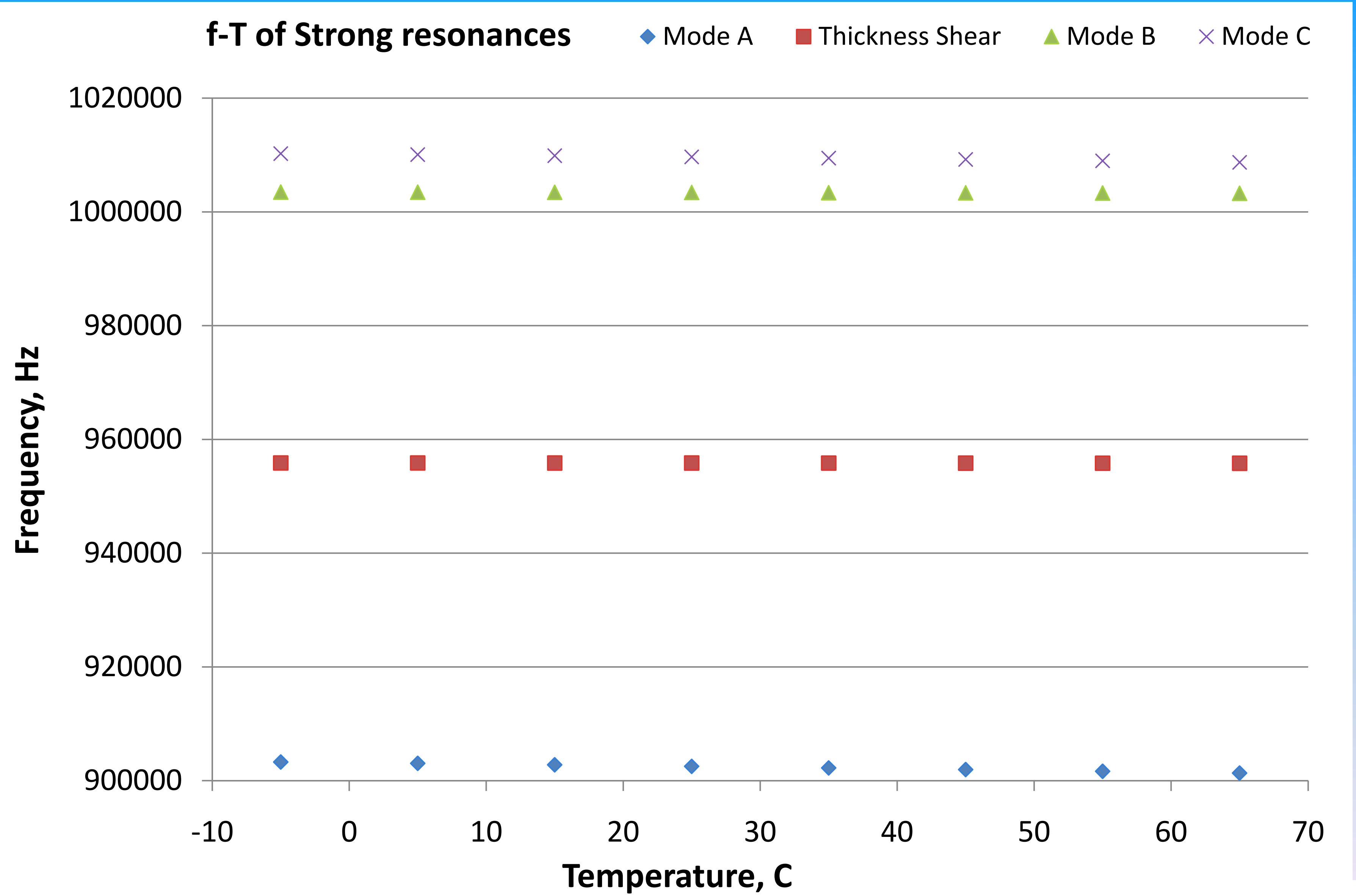

Sorting of modes according to frequency, x-y shear energy and current

- In experiments, only the strong resonances could be measured readily. These are modes that yield relatively large currents.
- We sort the modes according to the charge on the top surface of the plate. Strong resonances have relatively large charges.
- We sort the modes according to the x-y shear energy. The thickness shear mode has both large charge and large x-y shear energy.

Comparison of f-T model with Sekimoto's data for Mode A

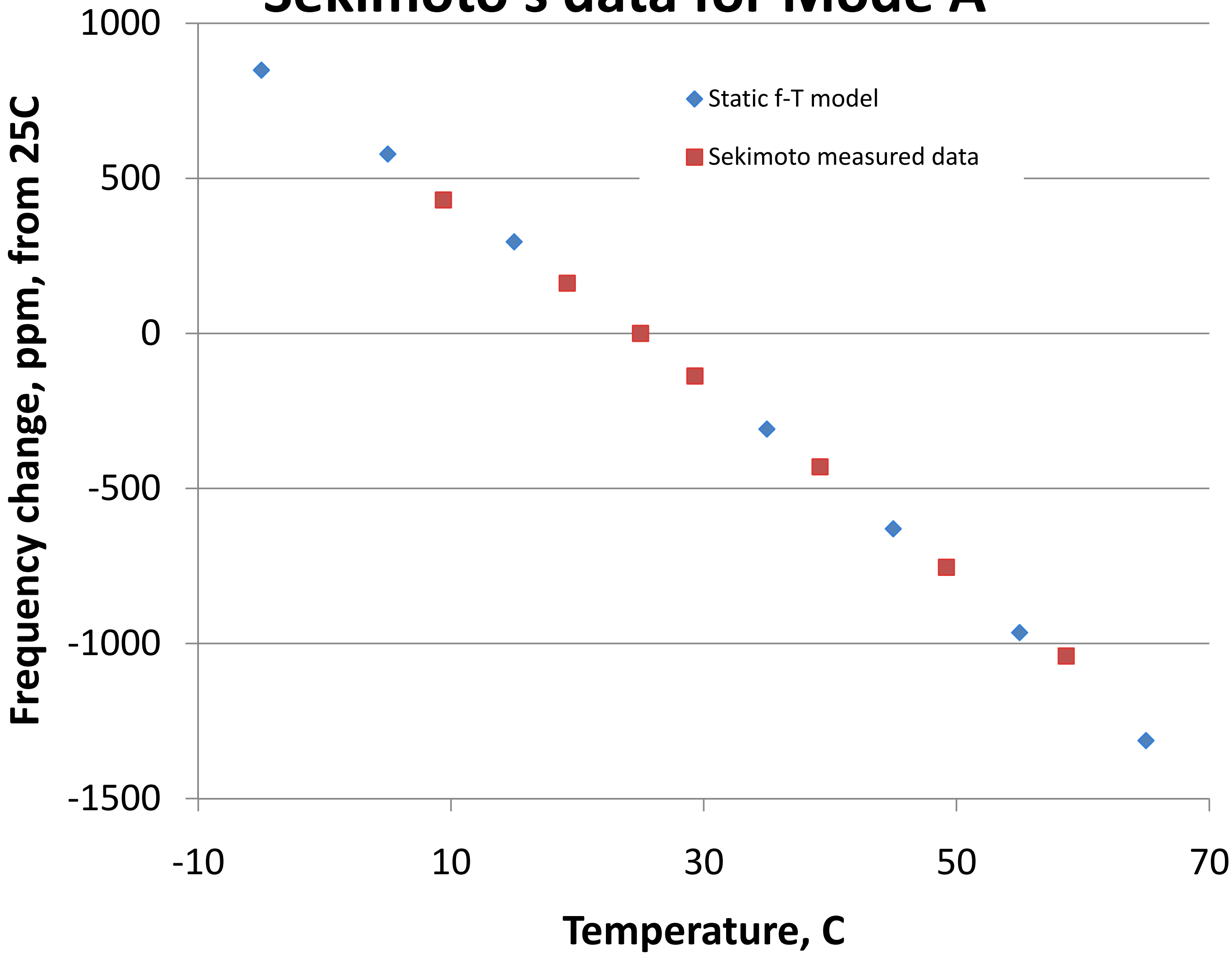

Comparison of f-T model with Sekimoto's data for the thickness shear mode

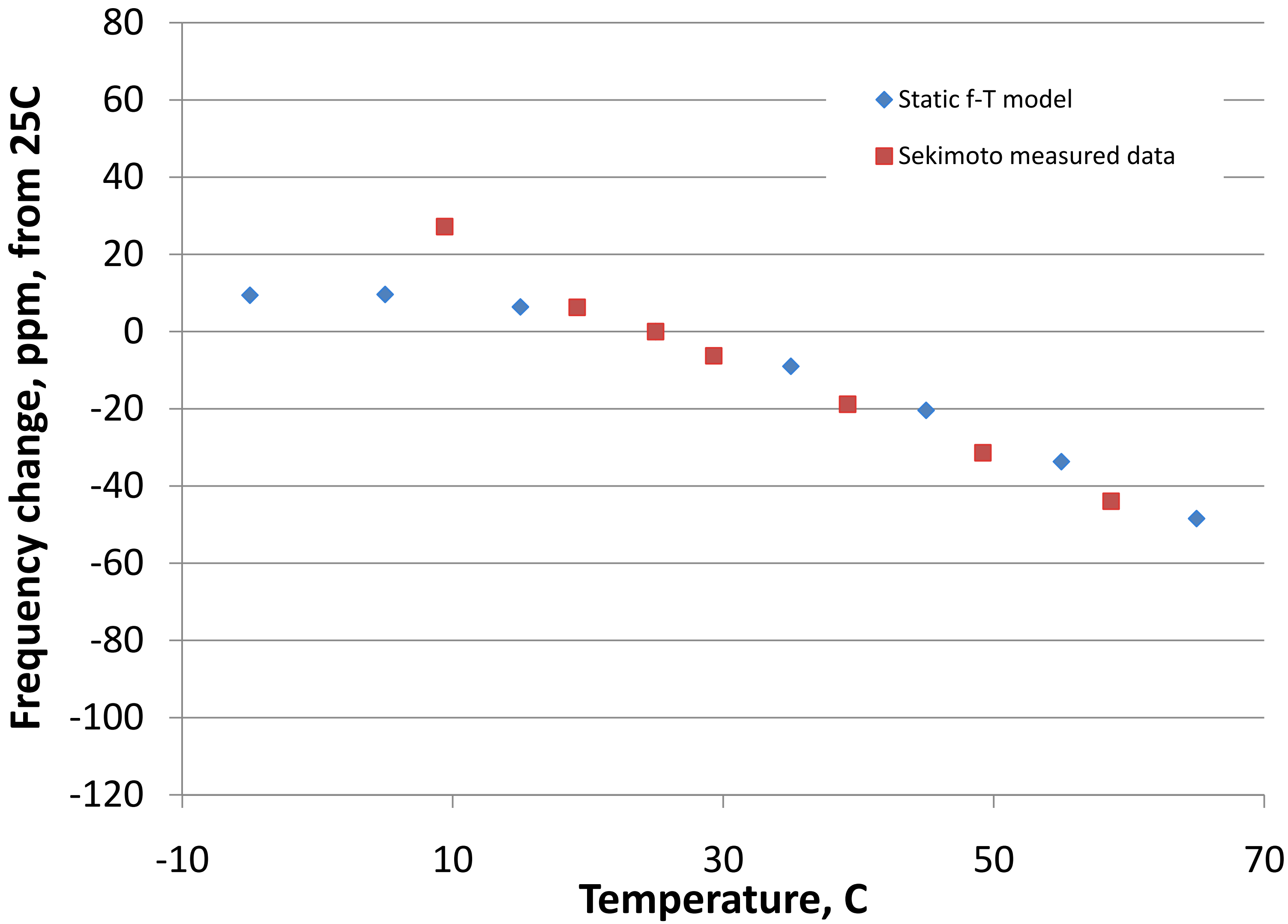

Comparison of f-T model with Sekimoto's data for Mode B

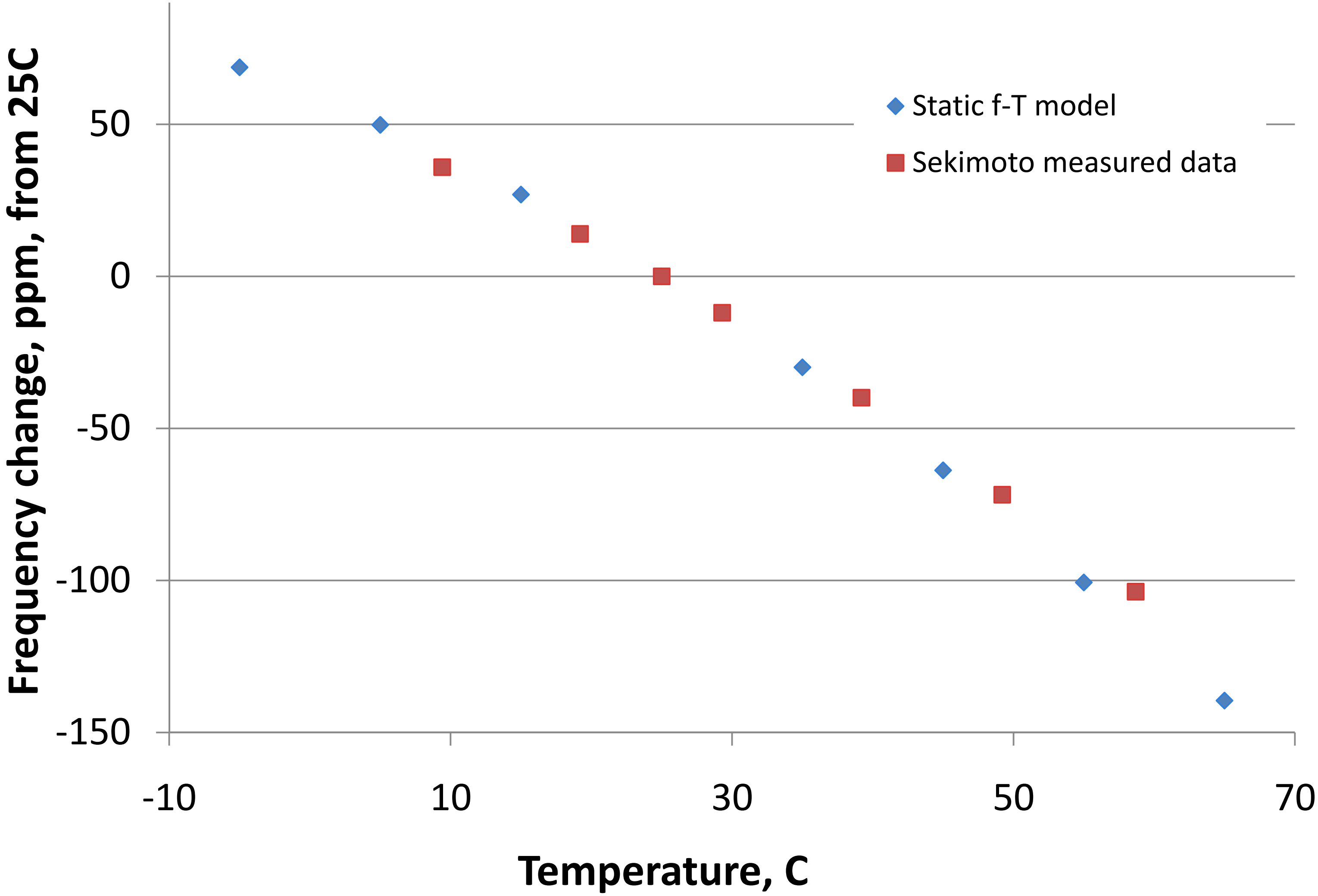

Comparison of f-T model with Sekimoto's data for Mode C

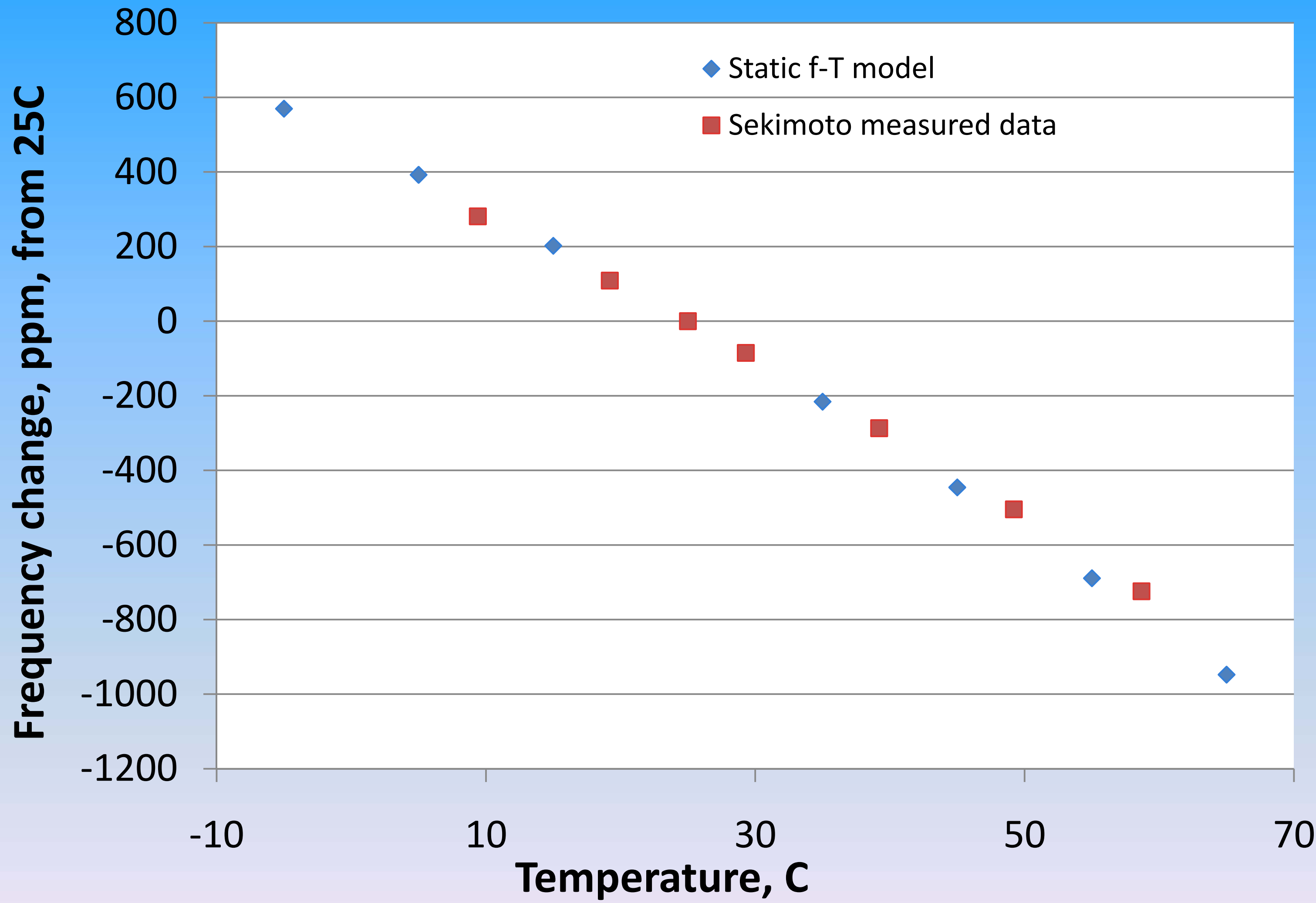

Thank you very much for participation!

Please send your comments, suggestions, and technical questions to

yyong@rci.rutgers.edu

wangji@nbu.edu.cn